

# Correlation of Load Bearing Tests on Soils

ROBERT L. KONDNER AND RAYMOND J. KRIZEK,  
*Civil Engineering Department, Technological Institute,  
Northwestern University, Evanston, Ill.*

Various load bearing test techniques are analyzed, both theoretically and experimentally, in an attempt to integrate the effects of the many variables that influence the bearing capacity and load-deformation characteristics of soils. Considerable use is made of the methods of dimensional analysis. The physical variables considered include the settlement or penetration of the loading plate or piston, applied force, size and shape of the plate or piston, method of testing, time of loading, number of load applications, and the properties of the soil being tested. Correlation between the load-deflection relations for load bearing tests and the soil stress-strain curves obtained from triaxial and unconfined compression tests are given. Laboratory and field data obtained from various locations throughout North America are analyzed and interpreted. Attention is given to the correlation of rigid plate bearing tests and the California bearing ratio test.

• A PARTICULAR FIELD of soil mechanics and highway engineering which has been a continual source of interest to numerous investigators is the determination of the bearing capacity of soils from load bearing plate tests. The problem of collecting, analyzing, correlating, and interpreting rigid bearing plate test data has long been open to much discussion and has been the motivation for numerous articles and several symposia in recent years. A satisfactory quantitative measure of the bearing capacity of soil masses has assumed increased significance in modern practical engineering.

The variables involved in this study are the size and shape of the bearing plate or piston, force applied, settlement or penetration, the number of load repetitions, time of loading, and characteristic strength and viscosity parameters of the soil. The data analyzed were obtained from vari-

ous laboratory and field locations throughout North America. The variables involved are subjected to a theoretical analysis to illustrate a rational approach to this complex problem and the laboratory and field results are employed to demonstrate the feasibility of such an approach. Finally, these results are interpreted to form a rational basis for the correlation of such data.

The initial problem encountered in the analysis of such a wide range of available test data is the extreme diversification of current load test procedures. One summary of a number of procedures is presented by Housel (1). It is not the intent of this paper to criticize these procedures but simply to comment in general on the variables involved in each and their influencing effects on the soil response as considered from a viscoelastic viewpoint. The difficulties of including these wide variations in the

test procedure in any systematic analysis become immediately evident. Furthermore, any attempt to bring the bearing capacity problem within the scope of laboratory analysis introduces additional complications. As stated by Terzaghi (2), an effort to solve a problem of this kind is "an attempt to uncover the responsible factors by isolating the variables and systematically determining their relative importance."

In an attempt to bring all these variables within the realm of realistic analysis, the authors have used the techniques of dimensional analysis. Such an approach enhances the inter-related transformations between laboratory models, field tests, and prototype response.

A second important element which has been found wanting in a large percentage of the literature is the inclusion of a representative soil strength parameter. Numerous attempts have been made to correlate tests on a wide range of soil types and consistencies and yet there is no measure of soil strength or consistency included. This factor alone magnifies considerably the problem involved in any attempt to correlate logically the various test procedures in which a soil strength parameter is certainly significant. Also along this same line, it appears that most tests are concluded too soon; large deformations are not obtained and it would certainly be desirable to attain the ultimate bearing capacity before the test is terminated. It is the opinion of the authors that a strength parameter for each soil is "built into" the shape of each curve obtained; that is, the shape of the curve will be dictated by the strength characteristics of the soil.

Another problem that has come through an examination of the literature is the inability of some authors to reproduce test results both in the laboratory and in the field, and the frequent incompatibility of a number

of the results obtained. An example of the former is given in Figure 1 which shows the stress-strain plot for three samples of the same silty clay when subjected to a laboratory triaxial test. The maximum stress obtained by Sample 1 is about twice that obtained by Sample 3. To illustrate the second case, Figure 2 shows two similar bearing plate tests which were performed on two cohesive soils having the same uniaxial stress-strain response; yet the one curve yields plate pressures approximately three times the other for comparable deflections. It is evident that information of this type can never be reconciled in any analysis.

This paper extracts data from numerous sources in the literature, disregarding the obvious cases already mentioned, rearranges this data into a more workable form by employing principles of dimensional analysis, and then proceeds to analyze systematically the results of various tests, including strength parameters deduced from the nature of the curve. These results are then interpreted and explained at length with the ultimate result being a strong foundation for an apparent correlation between several laboratory and field testing procedures.

#### THEORETICAL ANALYSIS

The methods of dimensional analysis have been very successful tools in the fields of hydraulics and fluid mechanics for a number of years, but they have not been extensively used in the fields of soil mechanics and highway engineering. The senior author has been applying nondimensional techniques to a variety of problems in soil mechanics (3 through 9) and has found these methods to be very valuable research tools for such an experimental field. Because of the complex viscoelastic properties of soils and the complicated interaction of soil-solid systems, it is felt that the use of nondimensional techniques

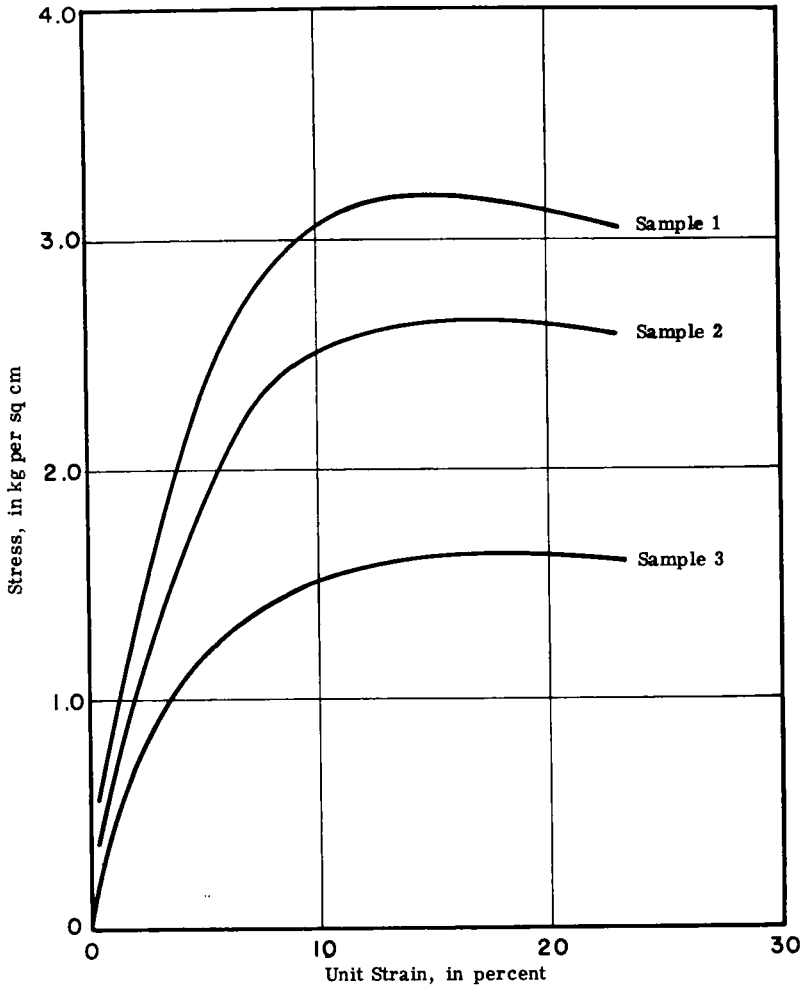


Figure 1. Stress-strain relationship, triaxial compression tests.

in both model and prototype research investigations offers definite advantages with regard to the cost, number of variables and conditions that can be studied, and time for completion of such studies.

Dimensional analysis offers a simple way to formulate a description, in functional form, of a physical phenomenon in terms of a finite number of physical quantities. Such methods, as used to formulate relationships among physical quantities, can be

briefly summarized. If there are  $m$  physical quantities containing  $n$  fundamental units, which can be related by an equation, then there are  $(m-n)$ , and only  $(m-n)$ , independent, nondimensional parameters, called  $\pi$ -terms, such that the  $\pi$ -terms are arguments of some indeterminate, homogeneous function  $\kappa$ :

$$\kappa(\pi_1, \pi_2, \pi_3, \dots, \pi_{m-n}) = 0 \quad (1)$$

The general methods of dimensional analysis have been described

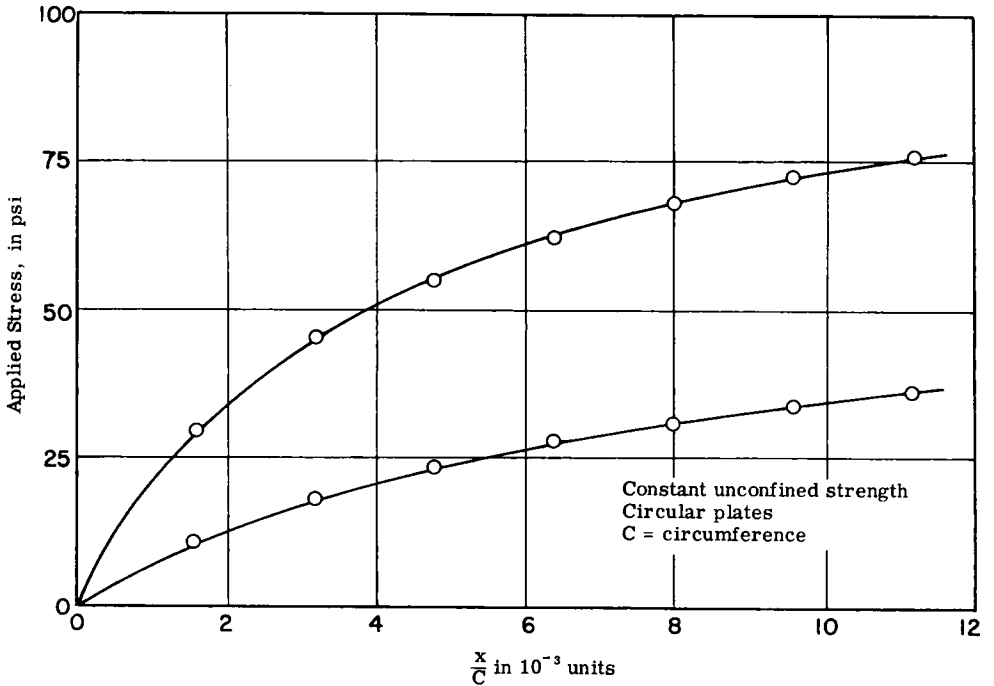


Figure 2. Comparison plot of bearing plate tests.

TABLE 1  
PHYSICAL QUANTITIES IN THE DIMENSIONAL  
ANALYSIS OF LOAD BEARING PLATE TESTS  
ON SOIL

Physical Quantity	Symbol	Fundamental Unit
Surface deflection or settlement	$x$	$L$
Applied force	$F$	$F$
Number of load applications	$N$	$FLT$
Cross-sectional area of plate	$A$	$L^2$
Perimeter of plate	$C$	$L$
Time of loading	$t$	$T$
Strength parameter of the soil	$q$	$FL^{-2}$
Viscosity of the soil	$\eta$	$FL^{-2} T$
Angle of internal friction	$\phi$	$FLT$

quantities considered are given in Table 1 using the force, length, and time system as fundamental units.

For the problem under consideration the applied surface tractions constitute the force system of primary interest and hence the body or gravity forces are not considered. It is assumed that the material constants needed to describe the deformation characteristics of the soil are, in general, implicit in a characteristic soil strength parameter, angle of internal friction, and effective soil viscosity. The characteristic soil strength parameter is quite general in nature, and may take the form of a shear or compression modulus, unconfined compressive strength, or a relaxation modulus function, depending on the circumstances under consideration. The angle of internal friction includes the frictional resistance of sands and mixed soils, and

elsewhere (10, 11) and the particular problems encountered in the soil mechanics field when applying this tool have been described in detail by Kondner (3, 4, 8, 9) and will not be repeated in this paper. The physical

the viscosity term controls the rate at which deformations take place in a soil. The duration of loading is important in creep and viscous response. The effect of the geometry of the bearing plate is expressed by the cross-sectional area and circumference. Some fatigue, strain hardening, and history effects are included in the number of load applications.

Because there are nine physical quantities and three fundamental units, there must be six independent, nondimensional  $\pi$ -terms. These  $\pi$ -terms can be methodically obtained by choosing  $n$  physical quantities (in this case, three) that contain all  $n$  fundamental units and cannot be formed into a nondimensional parameter by themselves (for example,  $F$ ,  $t$ , and  $q$ ) and combining them with each of the remaining quantities one at a time. Because of the great difficulty in experimentally determining the explicit form of the functional relation of Eq. 1, several modifications may be required in the form of the  $\pi$ -terms obtained. Because some of the requirements of the function  $\kappa$  are that it consist of independent nondimensional parameters, there is nothing unique about the forms of the  $\pi$ -terms. Therefore, it is possible to transform algebraically the  $\pi$ -terms in any way desired so long as the final  $\pi$ -terms are nondimensional and independent. Thus, the following  $\pi$ -terms can be obtained:

$$\pi_1 = \frac{x}{C}, \pi_2 = \frac{F}{Aq}, \pi_3 = \frac{C^2}{A}, \pi_4 = \frac{qt}{\eta} \text{ or } \frac{Ft}{A\eta},$$

$$\pi_5 = N, \text{ and } \pi_6 = \phi \quad (2)$$

The  $\pi$ -terms of Eq. 2 may be substituted into Eq. 1 to obtain the functional relationship which can be rewritten

$$\frac{x}{C} = \kappa \left( \frac{F}{Aq}, \frac{C^2}{A}, \frac{Ft}{A\eta}, N, \phi \right) \quad (3)$$

In Eq. 3 and hereafter,  $\kappa$  denotes "some function of" but not neces-

sarily the same function for each equation. This notation is used to avoid the use of numerous subscripts and superscripts as a means of differentiating between the equations.

The nondimensional  $\pi$ -terms may be interpreted in the following manner. The deflection or settlement parameter  $x/C$  is the dependent variable and is a measure of the amount of deflection under an applied load. The term  $F/Aq$  is the ratio of the applied stress to the resisting stress and is called the strength ratio. The strength ratio is analogous to the Cauchy Number in strength of materials and elasticity. The term  $C^2/A$  is a characteristic shape factor. For a circular cross-section of any size the shape factor is equal to  $4\pi$  ( $\pi = 3.1416$ ), and for a square shape the value is 16. The creep and viscous effects are included in the terms  $qt/\eta$  and  $Ft/A\eta$  which are considered to be proportional to the ratio of the time of loading to a characteristic relaxation time of the soil and is called the time ratio or time factor. The form  $Ft/A\eta$  can be considered as the ratio of the applied to viscous forces and may include non-Newtonian effects. Either of these last two terms controls the rate processes. The terms  $N$  and  $\phi$  are, by definition, nondimensional and their physical significance has been given.

#### EXPERIMENTAL RESULTS

Although the functional relationship given in Eq. 3 is reasonably general in that it includes clays, sands, and mixed soils, the determination of the explicit form of the function for such a general case would be extremely difficult. These difficulties are compounded because of the general lack of information on the strength characteristics of the soils for the great volume of field tests reported in the literature. Strength

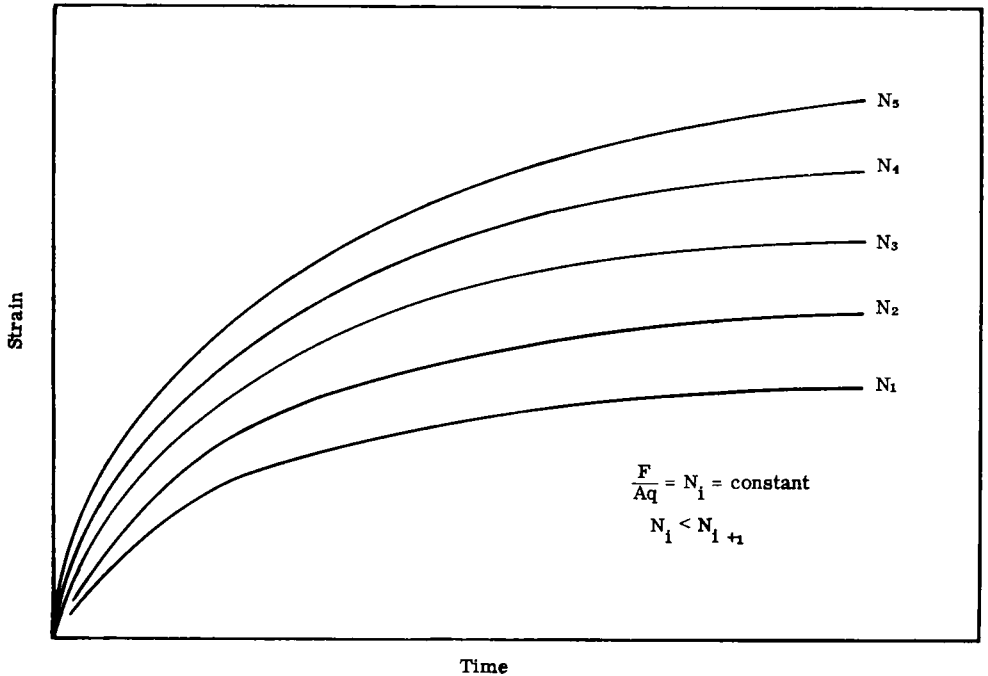


Figure 3. Typical soil creep response.

characteristics are of paramount significance and must be included in order to attempt any correlation among tests. Because of these difficulties, no attempt will be made to cross-correlate completely the various  $\pi$ -terms into an explicit form for Eq. 3.

#### Rate Effects

An equally important factor about which almost nothing is known is the soil flow characteristics that are included in the term  $Ft/A\eta$ . Examination of a tabular analysis of load test procedures given by Housel (1) and other authors indicates that most test loads are applied until the rate of settlement decreases to a specified value. It is well known that creep curves for soils are generally of the shape given in Figure 3. This shape applies for both laboratory stress-strain-time tests as well as bearing plate tests.

For a procedure with a constant terminal rate of settlement the value of  $Ft/A\eta$  may vary over an extremely wide range. In the case of a circular plate,  $C^2/A=4\pi$ , under a single load application,  $N=1$ , on a soil having a constant value of  $\phi$  which may or may not be zero, Eq. 3 may be written in the form

$$\frac{x}{C} = \kappa \left( \frac{F}{Aq}, \frac{Ft}{A\eta} \right) \quad (4)$$

In order to obtain a unique and compatible relationship between  $x/C$  and  $F/Aq$ , a constant value of  $Ft/A\eta$  is required for each load increment. As the applied load or stress increment,  $F/A$ , is increased, the time requirement to reach a constant settlement rate increases and the viscosity  $\eta$  tends to decrease; that is, the soil becomes "more fluid." Thus, the term  $Ft/A\eta$  increases very much

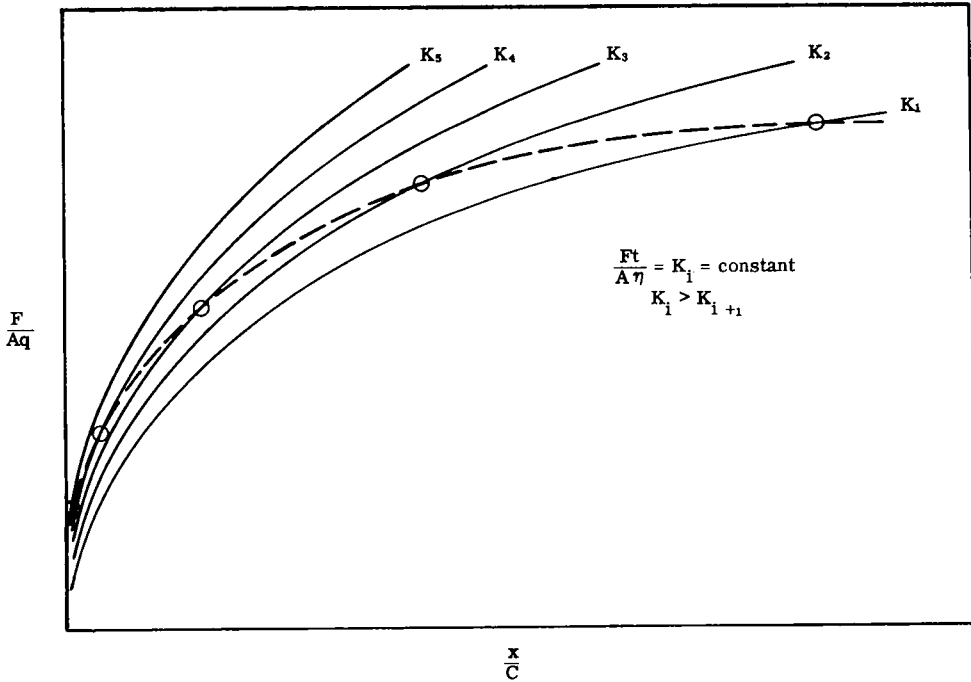


Figure 4. Influence of rate effects.

and the resulting curve relating  $x/C$  and  $F/Aq$  is much lower than the curve that would have been obtained had the initial value of  $Ft/A\eta$  been maintained constant. The results of such a hypothetical test are given in Figure 4 where the unique curves for constant values of  $Ft/A\eta$  are solid and the relation for the constant terminal rate of settlement test ( $Ft/A\eta$  variable) is given by the dashed line.

An even more difficult problem is the correlation of bearing plate tests on soils of considerably different consistencies or strengths; for example, on soft and stiff clays. For such soils, under constant applied stress, the viscosity  $\eta$  may differ by a factor of a hundred or more. Thus, compatible values of  $Ft/A\eta$  would be extremely difficult to obtain. The consistency effects on  $\eta$  are, in general, much

greater than non-Newtonian effects.

A more rational way to specify procedures would be with regard to  $Ft/A\eta$  by which stress increments and/or time intervals of loading could be adjusted to maintain compatibility. Unfortunately, the field of soil mechanics has not yet reached a state of development where such loading and time rates can be predicted. There is considerable need for more complete studies of the flow characteristics of soils.

#### *Applied Stress Intensity and Soil Strength*

In spite of the difficulties encountered because of viscous effects it is interesting to examine the results of studies conducted on circular plates,  $C^2/A=4\pi$ , in which  $N$  and  $\phi$  are constant and  $Ft/A\eta$  has been neglected

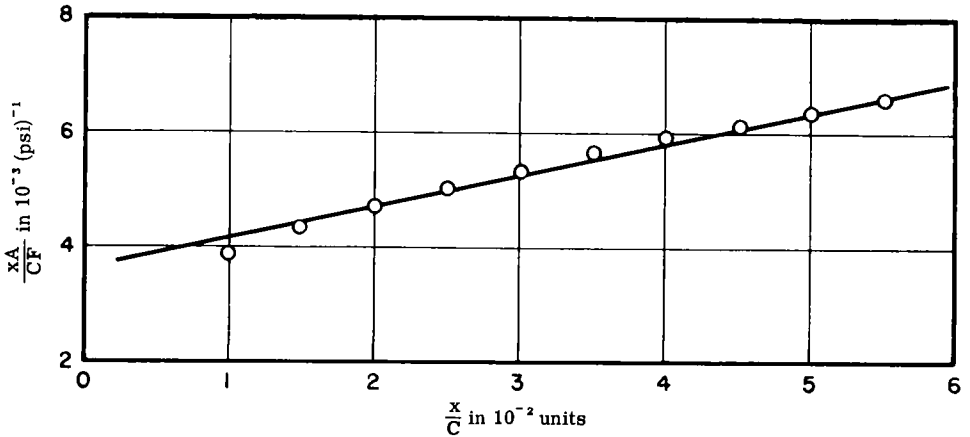


Figure 5. Model bearing plate tests on soft clay (Kondner and Krizek).

by necessity. For such cases the functional relation can be written as

$$\frac{x}{C} = \kappa \left( \frac{F}{Aq} \right) \quad (5)$$

A major difficulty in determining the explicit form of Eq. 5 from either new or previously reported experimental studies is the problem of defining and obtaining a satisfactory soil strength parameter  $q$ . It is the authors' contention that for a constant test procedure the shape of the curve of applied stress,  $F/A$ , vs deformation parameter,  $x/C$ , is uniquely dictated by the strength characteristics of the soil; that is, a strength parameter is "built into" the shape of the curve. In addition, if such a strength parameter is built into the shape of the curve, there must be a correlation between the stress-deflection relation for the bearing plate tests and the laboratory stress-strain relation.

*Model Studies.*—The first test results to be considered are those given by Kondner and Krizek (5) for model bearing plate tests on both soft and stiff clays. Because the strength parameter is assumed to be related to the shape of the stress-deformation

parameter curve, the use of a secant modulus seems to be a logical approach to the analysis. The  $F/A$  vs  $x/C$  data for various diameter circular plates on soft clay were obtained from Figure 7 (5). These data have been replotted in the form of the reciprocal of the secant modulus,  $xA/CF$ , vs  $x/C$  and are given in Figure 5. The straight line obtained thus indicates that the explicit form of the  $F/A$  vs  $x/C$  relation is a two-constant hyperbolic equation and can be written as

$$\frac{xA}{CF} = a + b \frac{x}{C} \quad (6)$$

or

$$\frac{F}{A} = \frac{\frac{x}{C}}{a + b \frac{x}{C}} \quad (7)$$

where  $a$  and  $b$  are the intercept and slope, respectively, obtained from Figure 5. The initial slope of the  $F/A$  vs  $x/C$  curve is  $1/a$  and the ultimate or "yield" stress  $(F/A)_{ult}$  is  $1/b$ .

A similar analysis was made on the stress-strain curve obtained in unconfined compression for the soft clay and is given in Figure 6 in the form



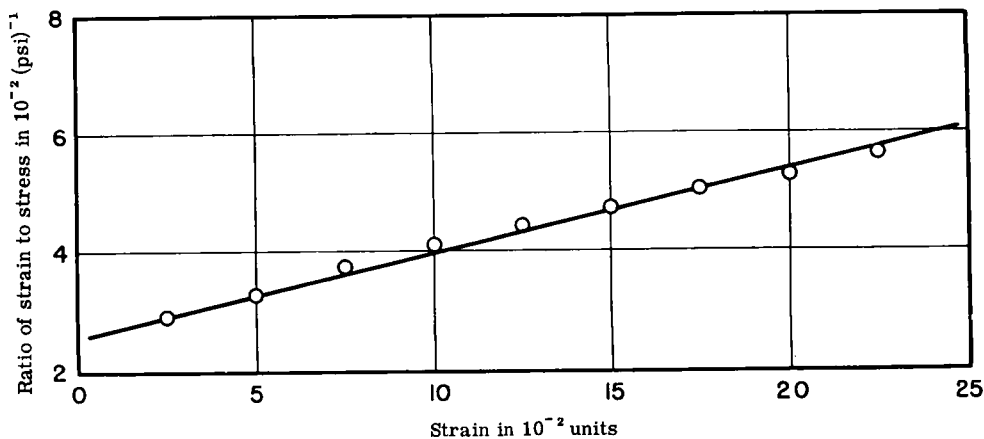


Figure 6. Stress-strain curve for soft clay (Kondner and Krizek).

of the reciprocal secant modulus, ratio of strain  $\epsilon$  to stress  $\sigma$ , vs the strain. The straight line obtained indicates that the stress-strain relation is also a two-constant hyperbolic equation and, similarly, can be written as

$$\sigma = \frac{\epsilon}{a + b\epsilon} \quad (8)$$

where  $a$  and  $b$  are the intercept and slope, respectively, obtained from Figure 6. Because  $1/b$  is equal to  $\sigma_{ult}$ , it must be proportional to the maximum unconfined compressive strength,  $q_u$ , of the soil. Comparison of Eqs. 7 and 8 indicates that  $F/A$  is analogous to  $\sigma$  and  $x/C$  corresponds in some manner to  $\epsilon$ . Thus, the similarity of Figures 5 and 6 and Eqs. 7 and 8 seems to substantiate the authors' contention of a "built-in" strength parameter for the bearing plate test. A detailed study of the explicit form of the correlation with the laboratory stress-strain relation is beyond the scope of this paper, but such a study will be conducted in the near future.

The results of similar tests of model circular bearing plates of vari-

ous diameters on a stiff clay were obtained from Figure 8 of a paper by Kondner and Krizek (5). These results have been replotted in the form of  $xA/CF$  vs  $x/C$  and are shown in Figure 7. The two-constant hyperbolic form of Eq. 7 is obtained where  $a$  and  $b$  are the intercept and slope, respectively, obtained from Figure 7. The unconfined compression stress-strain relation for the stiff clay is given in Figure 8 in the form of  $\epsilon/\sigma$  vs  $\epsilon$  and takes the hyperbolic form of Eq. 8. Thus, the strength parameter correlation seems to be valid for a wide range of soil consistencies for small-scale model tests.

*Field Studies.*—The correlation between load bearing tests and laboratory unconfined compression tests that has been presented for model studies will be extended to cover field studies.

*Subsurface Tests on a Chicago Clay.*—The first field study to be considered was conducted by Dix and Lukas (12). Three circular plate bearing tests were performed on a Chicago clay at depths of 20 to 30 ft below the ground surface. A summary of the plate sizes and depths are given in Table 2.

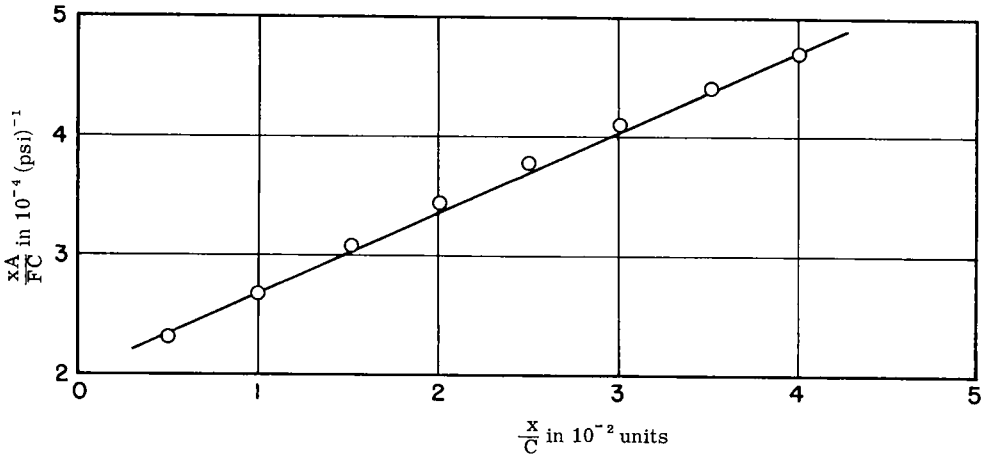


Figure 7. Model plate tests on stiff clay (Kondner and Krizek).

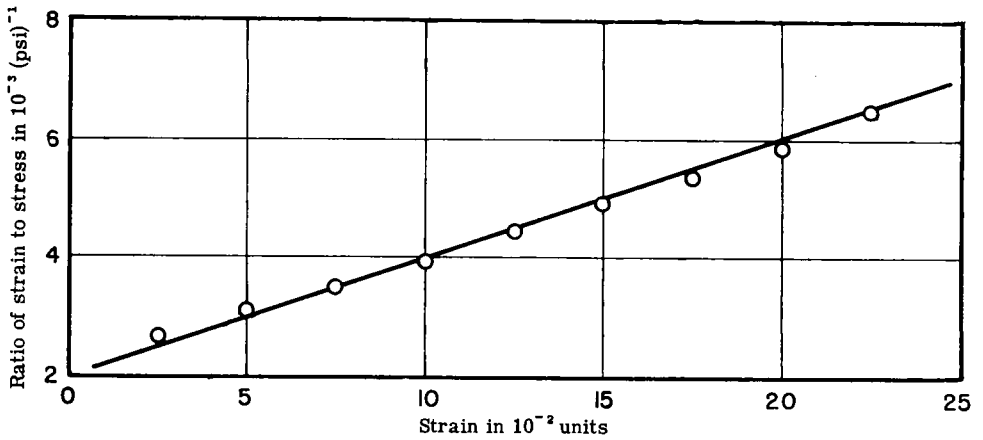


Figure 8. Stress-strain curve for stiff clay (Kondner and Krizek).

The basic test data are shown in Figure 9 by the solid curves in the form of applied stress vs deflection. Test 3, which has the largest diam-

TABLE 2  
PLATE SIZES AND DEPTHS, FIELD TESTS

Plate Test	Diameter of Plate (in.)	Cross-Sectional Area (sq ft)	Depth Below Ground Surface (ft)
1	13.5	1.00	20.6
2	24.0	3.14	23.0
3	30.0	4.91	27.0

eter plate and greatest depth below the ground surface, starts with the highest stress per unit deflection and then crosses and remains lower than the curve for Test 2, indicating experimental difficulties. The test data were replotted in the form of the reciprocal of the secant modulus,  $xA/CF$ , vs  $x/C$  and shown in Figure 10. Once again the two-constant hyperbolic form of Eq. 7 is obtained.

Both unconfined compression and triaxial compression test results have been replotted in Figures 11 and 12,

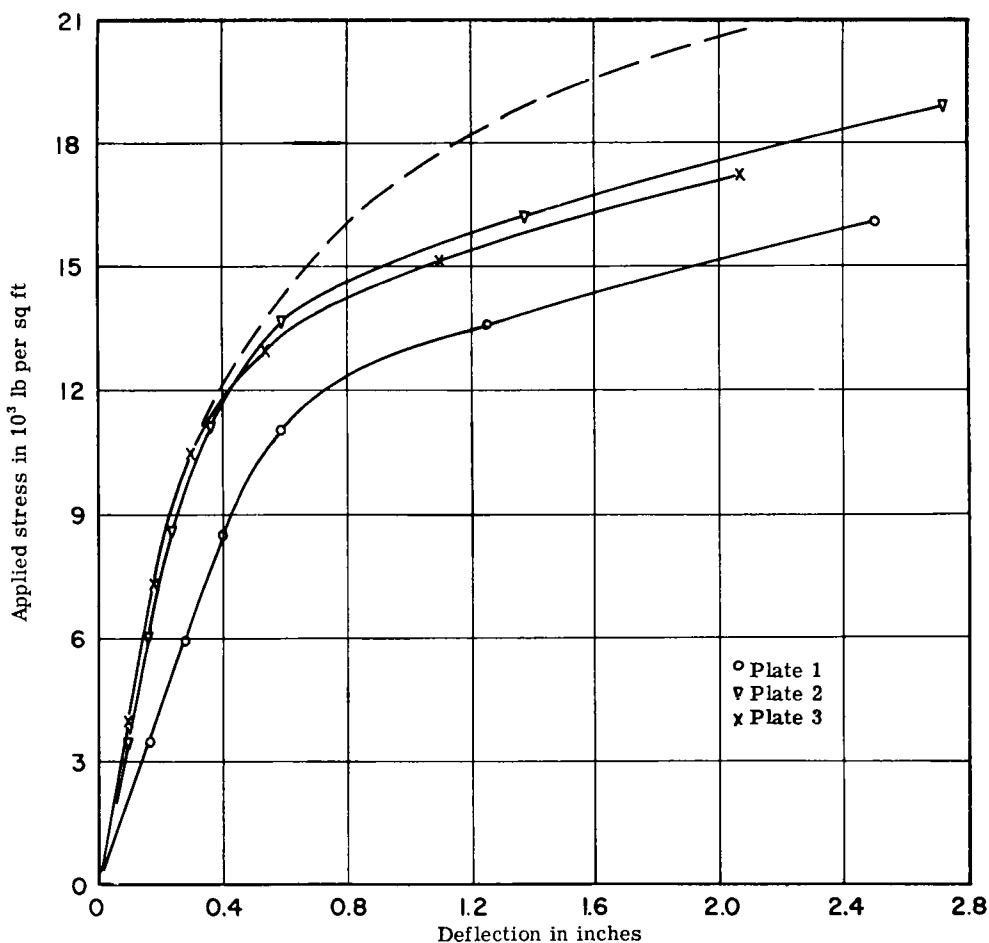


Figure 9. Bearing plate tests (Dix and Lukas).

respectively, in the form  $\epsilon/\sigma$  vs  $\epsilon$ . Once again the stress-strain relations take the form of Eq. 8. Tests 2 and 3 of Figure 10 show the same results although, as shown in Figures 11 and 12, the soil strength was greater under Test Plate 3. By relating the slopes,  $b$ , of Figure 10 with the strength curves it is possible to show that Test 3 should have followed the dashed curve of Figure 9. A complete discussion of this point is beyond the scope of the present paper.

Bearing Plate Tests.—The model

tests by Kondner and Krizek (5) and the field tests of Dix and Lukas (12) have shown the correlation between the stress-strain plots for conventional strength tests and bearing plate tests. To illustrate the general nature of the two-constant hyperbolic form of Eq. 7, the following series of test results have been analyzed.

The test data reported by Benkelman and Williams (13) for circular plates with diameters ranging from 1 to 7 ft, conducted on subgrades at the Hybla Valley test track near

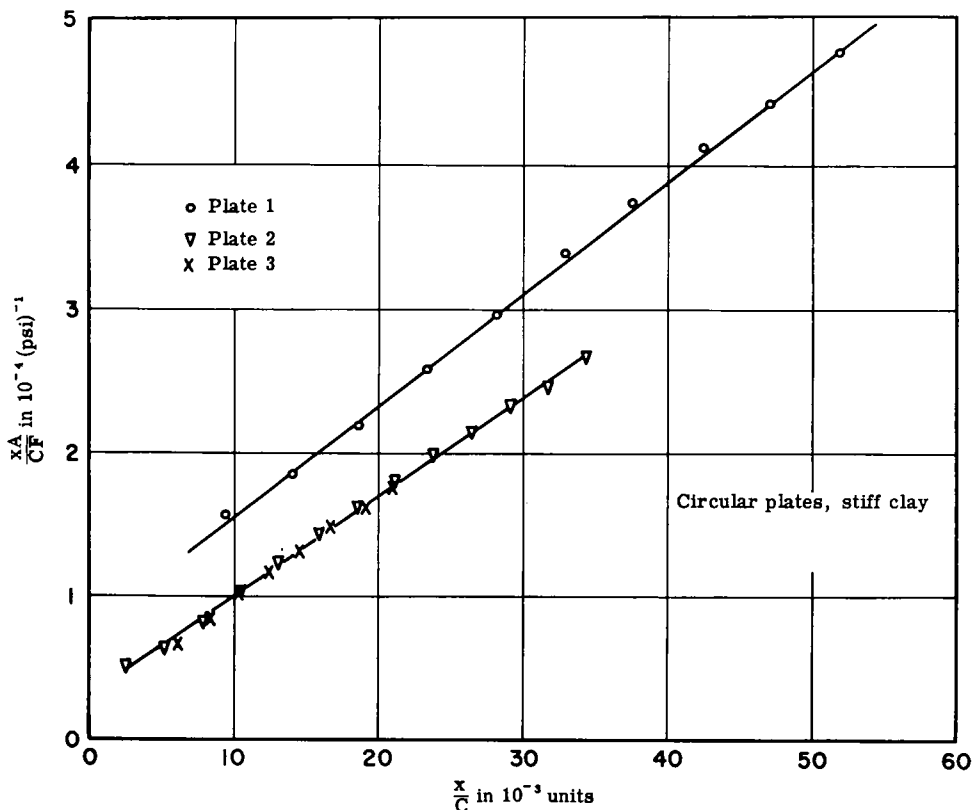


Figure 10. Bearing plate tests (Dix and Lukas).

Alexandria, Va., have been replotted and are shown in Figure 13. The hyperbolic fit is quite good.

Test data presented by Osterberg (14) on bearing plate tests on silty clay and buckshot clay conducted by the U. S. Army Engineers, Waterways Experiment Station, Vicksburg, Miss., are shown in Figures 14 and 15. Additional data given by Osterberg (14) on tests conducted at Wright Field and by Teller and Sutherland are shown in Figures 16 and 17.

Tests reported by McLeod (15) for circular plates of various diameters are given in Figure 18 in the form of applied stress,  $F/A$ , vs  $x/C$ . According to McLeod, the data given in the figure are typical of that obtained

for eight different airfields located throughout Canada. Figure 19 is a plot of  $xA/CF$  vs  $x/C$  and fits the form of Eq. 7.

Additional hyperbolic fits of bearing plate data are given in Figures 20 and 21 for circular plates tested on a slightly plastic blue clay and a stiff sandy blue clay by Housel.

#### California Bearing Ratio Tests

Because the California bearing ratio test is a particular type of load bearing plate test, such tests should also give applied stress vs deformation parameter relations similar to those obtained for the model and field studies previously presented. Figures 22 and 23 show the results of two

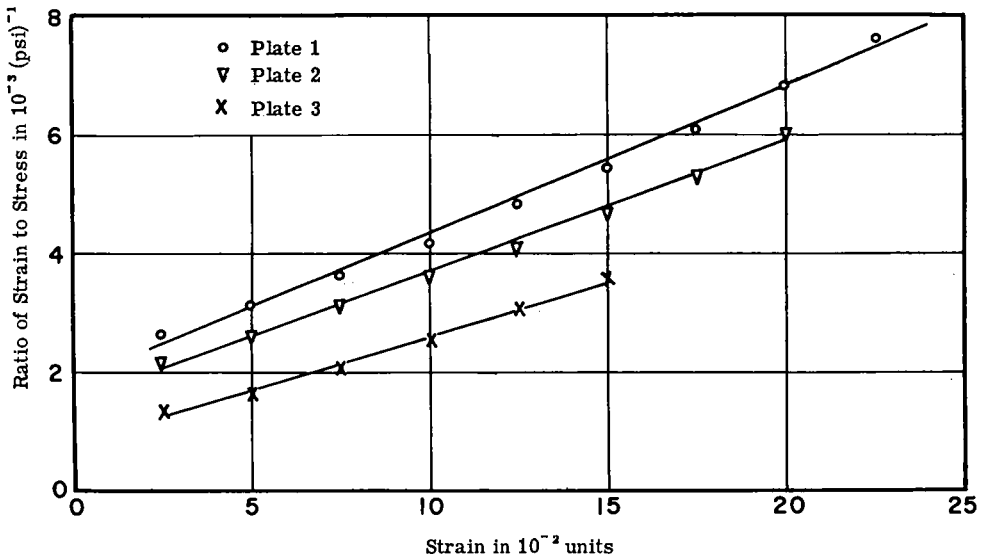


Figure 11. Unconfined compression tests (Dix and Lukas).

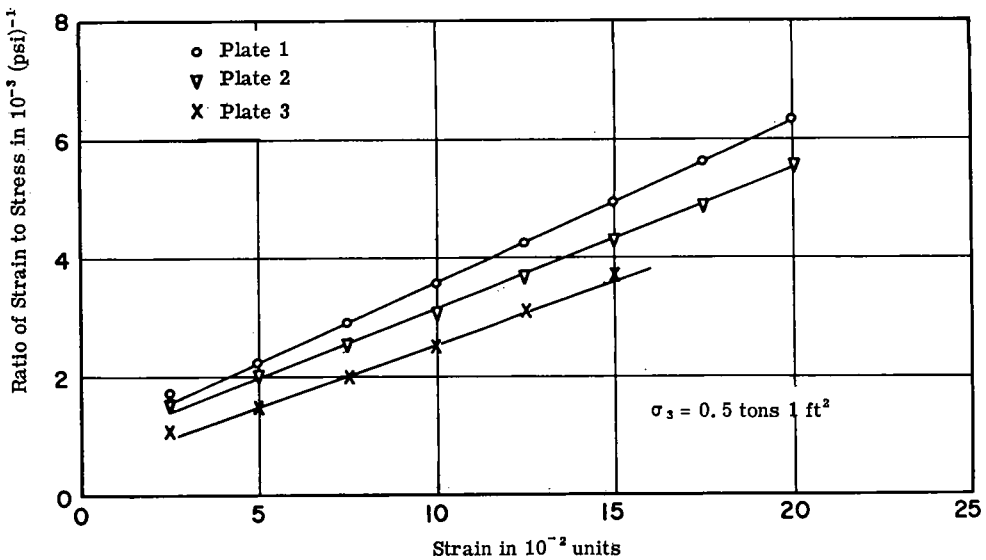


Figure 12. Triaxial compression tests (Dix and Lukas).

CBR tests conducted on a sandy loam soil and a clay loam given by Porter (16). Once again the hyperbolic forms of Eq. 7 are obtained. In addition, the standard 100 percent CBR

curve for crushed stone can also be represented by Eq. 7 as shown in Figure 24. Comparison of laboratory stress-strain tests and bearing plate tests for the model and field studies

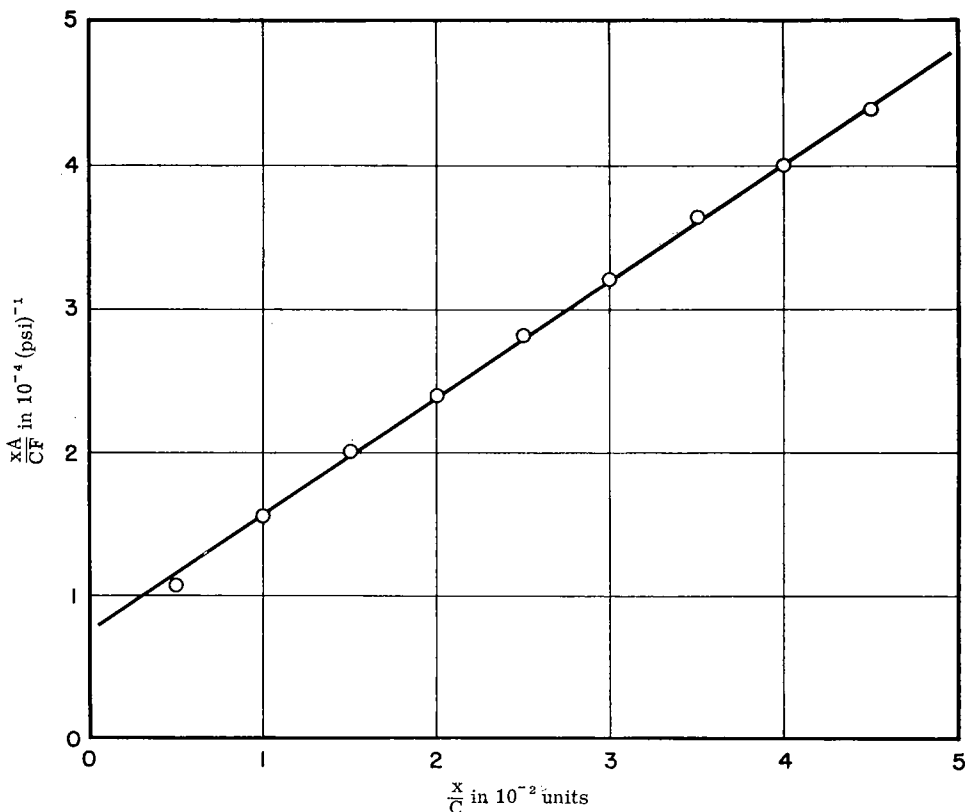


Figure 13. Bearing plate tests (Benkelman and Williams).

indicates that the CBR test is a measure of the soil strength, and as such, the CBR value is a ratio of the soil strength parameter to the strength parameter of a standard material (namely, crushed stone) at a particular value of  $x/C$ . It is important that the correlation between CBR values and bearing plate tests be made at compatible  $x/C$  values and not at equal values of  $x$ .

#### Shape Effects

The influence of the shape of a bearing plate on the applied stress vs deflection relation is included in Eq. 3 by the term  $C^2/A$ . Neglecting viscous, repetitional, and internal friction effects, the plate load-deflec-

tion-shape relationship as given by Eq. 3 can be written as

$$\frac{x}{C} = \kappa \left( \frac{F}{Aq}, \frac{C^2}{A} \right) \quad (9)$$

To determine the effect of shape on the variation of  $x/C$  as a function of the strength ratio,  $F/Aq$ , a series of tests were conducted on model plates of equal cross-sectional area, but with different values of  $C^2/A$ , on soils having approximately the same unconfined compressive strengths. The model plates used are shown in Figure 25. The cross-sectional areas of all of the plates were 2 sq in., but the values of  $C^2/A$  ranged from the geometric minimum of  $4\pi$  for the circular shape to a value

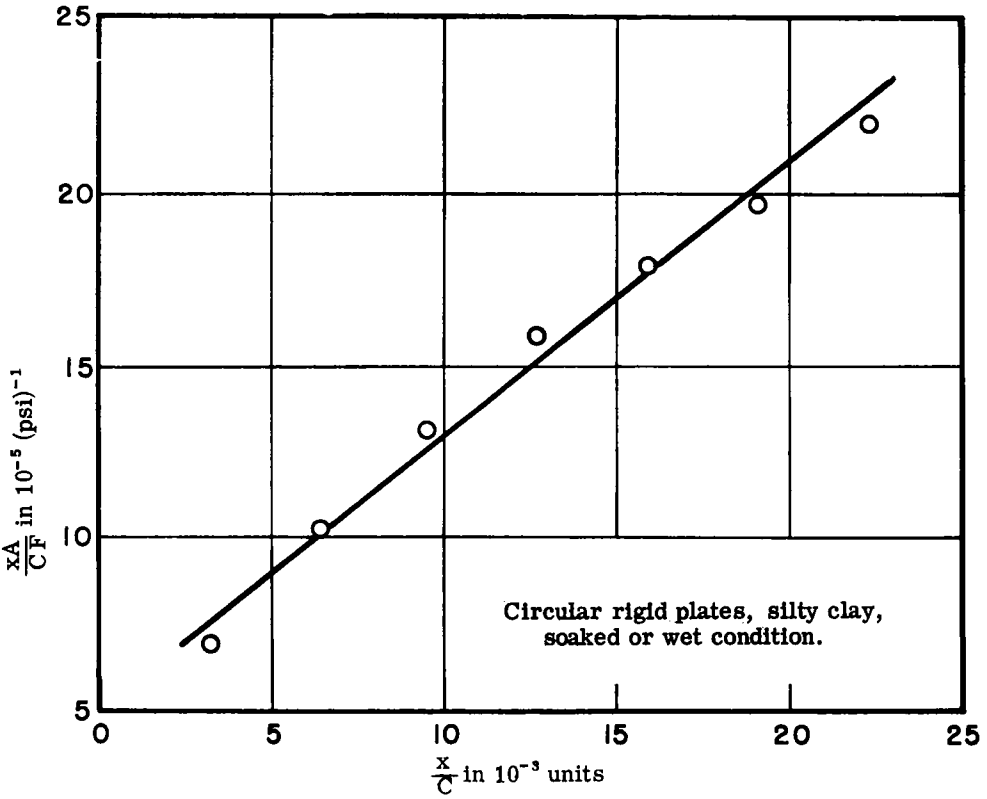


Figure 14. Tests by U. S. Waterways Experiment Station.

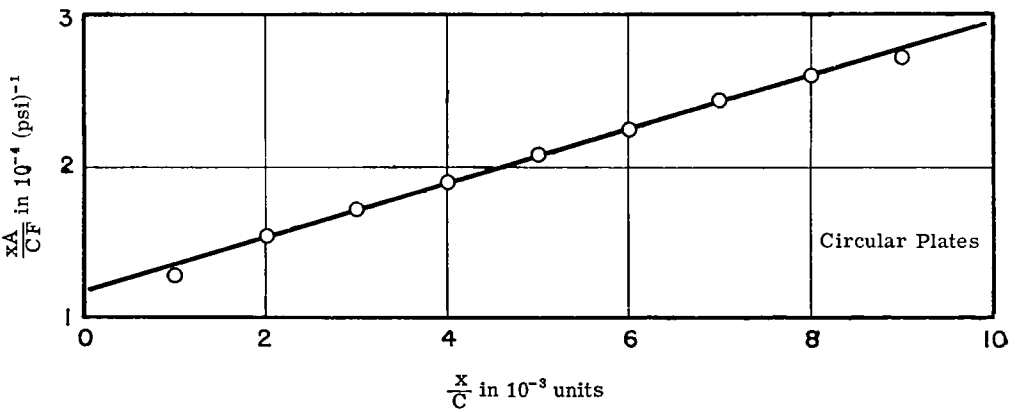


Figure 15. Bearing plate tests on buckshot clay (U. S. Waterways Experiment Station).

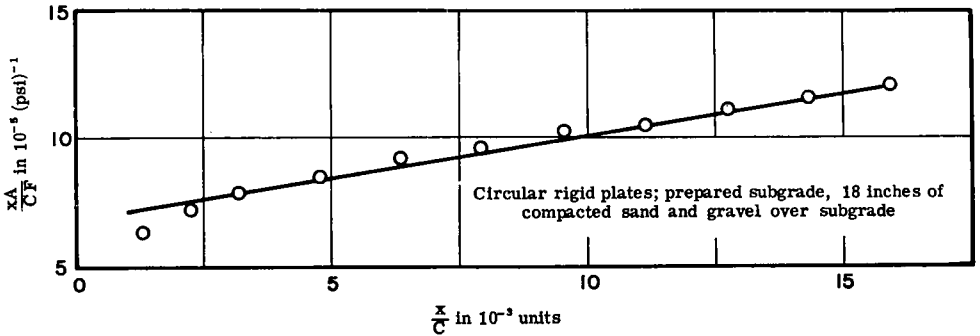


Figure 16. Average curve, Wright Field tests (U. S. Engineers, 1942).

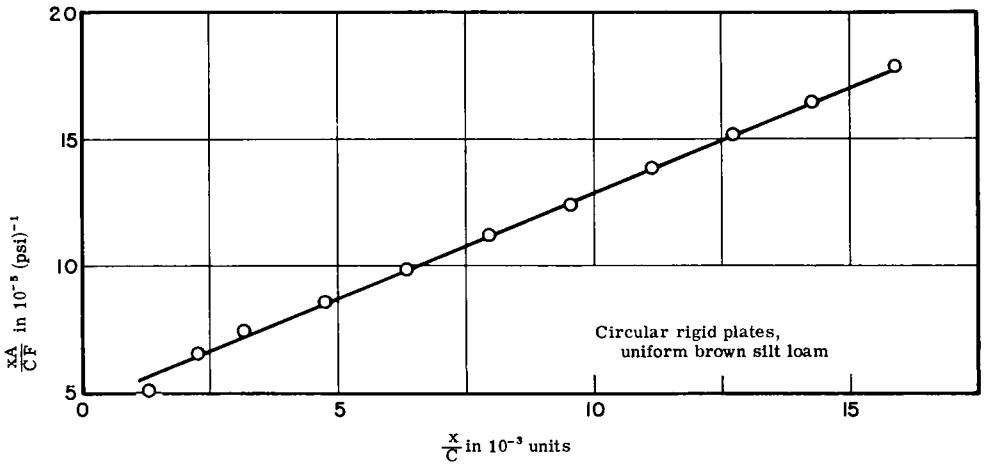


Figure 17. Average curve, tests by Teller and Sutherland, Series 3.

of 136 for the cross-shaped plate. The results of these tests are shown in Figure 26 where  $F/Aq$  has been plotted against  $x/C$  for various values of  $C^2/A$ . The strength parameter,  $q$ , used in Figure 26 is the unconfined compressive strength of the soil. Figure 26 shows a definite phenomenological influence caused by  $C^2/A$ . For a constant applied stress,  $F/A$ , the deflection parameter,  $x/C$ , increases for decreasing values of  $C^2/A$ . In comparing the results obtained using square plates of width  $b$  and circular plates of diameter  $d$  for equal cross-sectional areas on the

same soil, the plotting of  $x/b$  and  $x/d$  instead of  $x/C$  can lead to the following difficulty. For constant values of  $x/C$ , the ratio of  $x/b$  to  $x/d$  is 1.273. Because the deflection parameter in Figure 26 for the circular plate is approximately 18 percent greater than the square plate, a plot of  $F/A$  vs  $x/b$  or  $x/d$  would reverse the order of the two curves by approximately 9 percent. Considering the fairly high experimental error involved in field bearing plate testing, it seems quite possible that the correlation of the results of tests for a limited number of circular



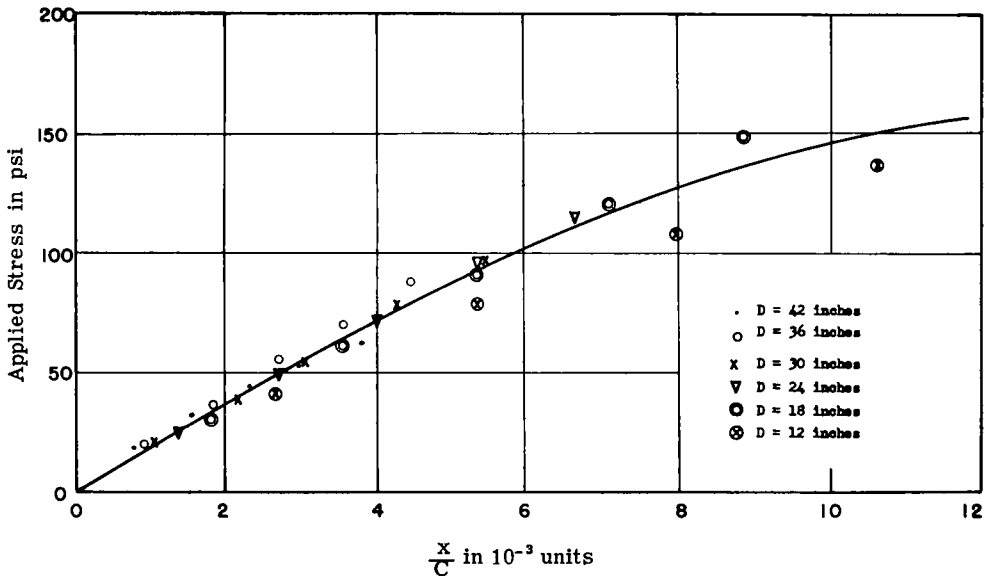


Figure 18. Typical bearing plate tests (McLeod).

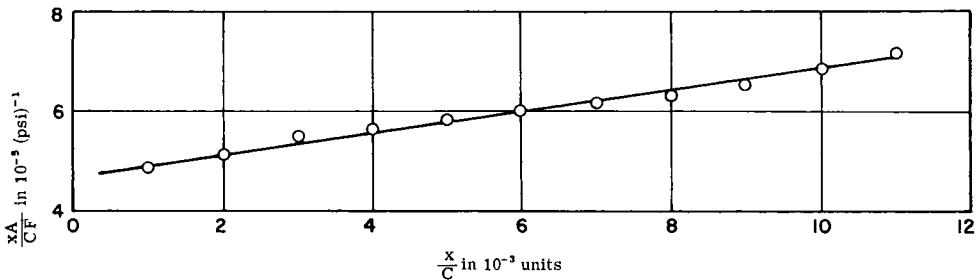


Figure 19. Typical bearing plate tests (McLeod).

and square plates would be inconclusive.

*Correlation of Various Strength Indexes*

In an attempt to draw some correlation between plate bearing tests and field California bearing ratio, cone-bearing, and Housel penetrometer tests, McLeod (15) has conducted an extensive testing program on cohesive soils at eight different airports located throughout Canada.

These locations are Ft. St. John, Grande Prairie, Saskatoon, Lethbridge, Dorval, Winnipeg, Malton, and Regina. The plate tests were performed on a 30-in. diameter plate with 10 repetitions of the load, and the other tests were conducted in accordance with standard procedures. The results of this work as reported by McLeod are in the form of subgrade support, in pounds, for 0.2-in. deflection vs representative indexes for each particular test. McLeod fitted each set of data with a

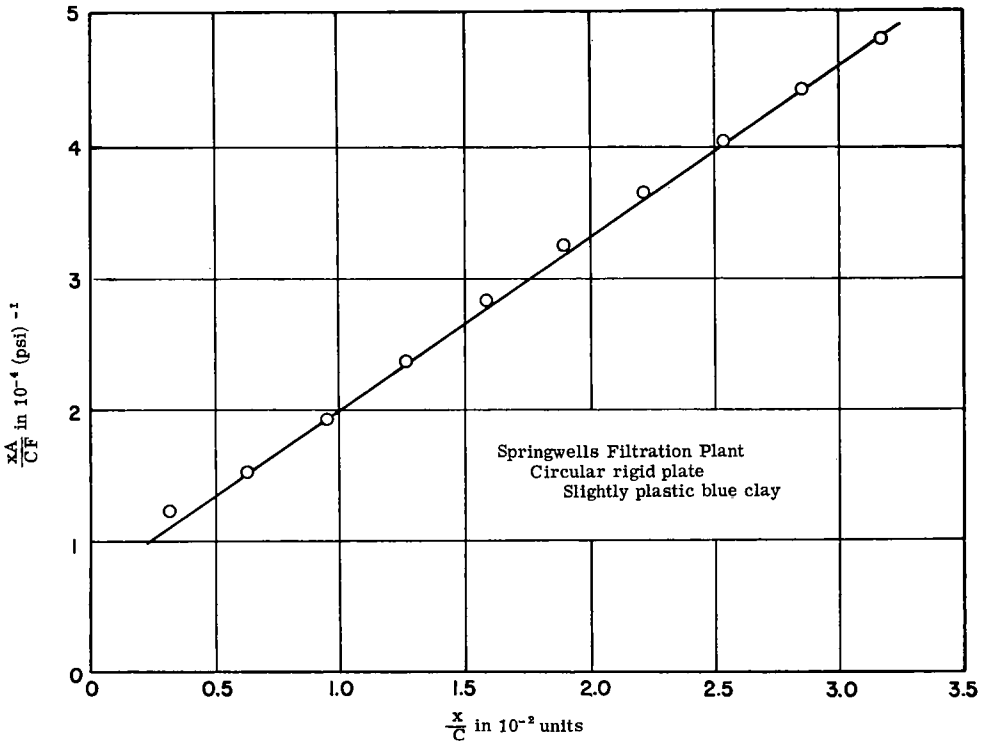


Figure 20. Bearing plate test (W. S. Housel).

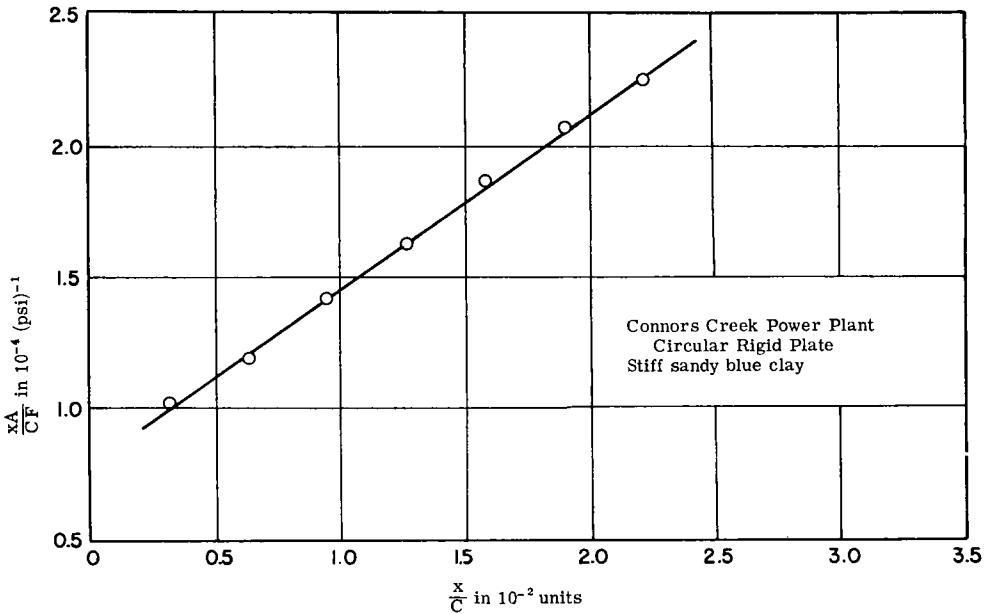


Figure 21. Bearing plate test (W. S. Housel).

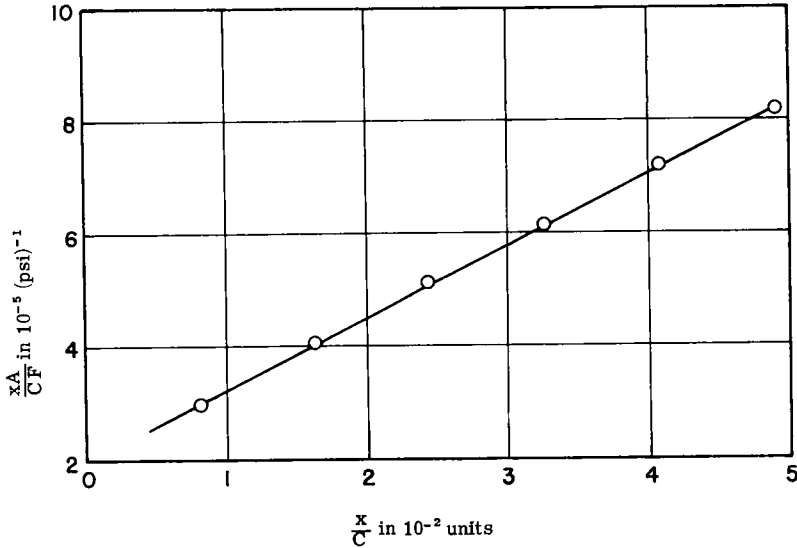


Figure 22. Typical CBR test on sandy loam soil (O. J. Porter).

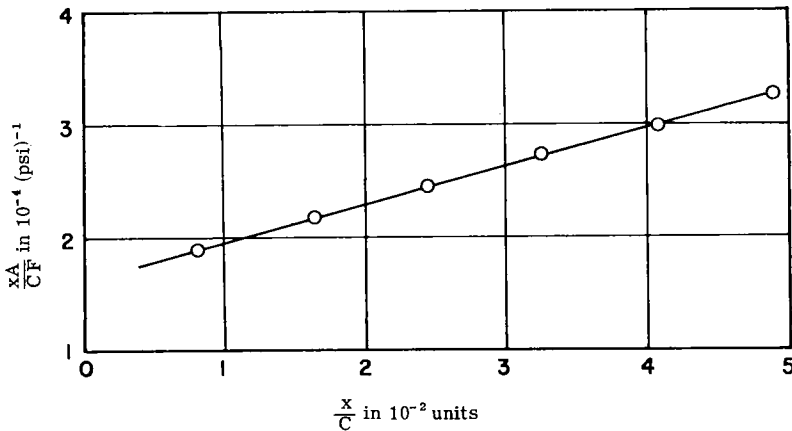


Figure 23. Typical CBR test on clay loam (O. J. Porter).

particular straight line and then correlated the straightline fits of the four types of test.

It has been observed that these same data can, in each case, be fitted reasonably well with a hyperbola. The curve for the field California bearing ratio data is shown in Figure 27; for cone-bearing, in Figure 28; and for the Housel penetrometer, in

Figure 29. By referring to the hyperbolic test plot in Figure 30 for each of these three cases, it is seen that each set of data reduces to the same hyperbola when the abscissa scale is appropriately selected. This establishes a correlation on a somewhat different basis than McLeod and exemplifies the possible hyperbolic nature of this wide range of data.

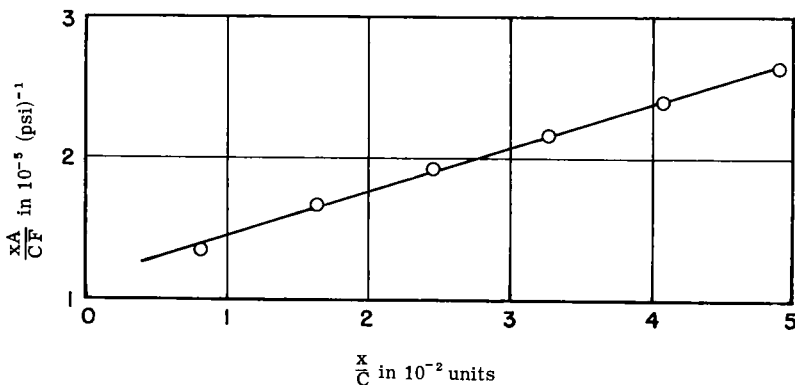


Figure 24. Standard CBR test.

The large scatter in McLeod's data as shown in Figures 27 through 29 is probably due to the wide variation in soil types and consistencies tested and to the fact that although the  $x/C$  values are constant for each index parameter, the viscosity and strength parameters have been neglected for the reasons previously discussed.

#### *Repetitional Loading*

At present most methods of pavement design are based on some index of soil strength obtained from tests in which the magnitude of the load is increased slowly and allowed to remain for some specified period of time or until some specified rate of deformation is reached. The results of such tests have been correlated empirically with soil performance and provide a reasonably reliable basis for design criteria.

The problem of repetitional loading of a soil mass, however, introduces additional variables into the analysis, and it does not follow that soil strength indexes obtained from normal static tests will provide a realistic measure of soil performance when subjected to repeated loads. A comprehensive rational approach to this problem should include not only the magnitude of the applied stress but also the number of applications,

frequency, and duration. To analyze in detail the effects of the latter two factors on the deformation and strength characteristics of a soil is beyond the scope of this paper and comment will be restricted to a brief presentation of the results obtained by other investigators. The subject of number of stress applications will be analyzed in some detail, and certain observations and correlations will be pointed out. A procedure for including this variable in a general force-deformation equation will be presented.

Seed and Chan (17) have shown that the duration of repetitional load tests may be very important in some soils due to an increase in thixotropic effects with time. These effects become increasingly significant at smaller strains and thixotropic stiffening appears to have greater effects in these tests than in the normal type of strength tests.

The results of numerous tests by Seed, Chan, and Monismith (18) on partially saturated specimens of silty clay subjected to repeated applications of a constant stress in triaxial compression indicate that up to at least 100,000 stress applications, deformation is independent of frequency within the range of 3 to 20 applications per min (and possibly as low as 1 application per min) and

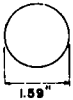
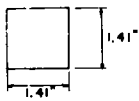
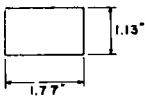
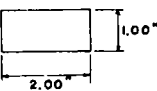
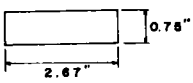
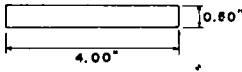
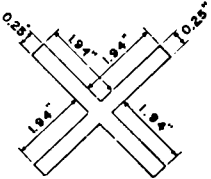
Plots	C	A	$\frac{C^2}{A}$
	5.00	2.0	4π
	5.66	2.0	16
	5.80	2.0	16.8
	6.00	2.0	18
	6.83	2.0	23.4
	9.00	2.0	40.5
	16.5	2.0	136

Figure 25. Plates of constant area and variable perimeter.

relationship. The validity of such an assumption has been questioned by McLeod (15) when he points out that the exponential relationship holds reasonably well up to 100 repetitions of load although "the direction of the curve has become somewhat uncertain for the last ten or fifteen repetitions."

One source of data for bearing plates subjected to repeated loads was found in McLeod (15) where a 30-in. diameter plate was subjected to 100 applications of a 40,000-lb load. These data have been subjected to the hyperbolic test plot shown in Figure 31 and found to satisfy the requirements for a hyperbola, and can be written as

$$\frac{x}{C} = \frac{N}{660 + 217N} \text{ for } 5 \leq N \leq 100 \quad (10)$$

Inasmuch as it has been shown previously in the case of the normal plate tests that there is a relationship between field plate bearing tests and laboratory stress-strain compression tests, it seems reasonable at this point to investigate the behavior of a laboratory specimen subjected to a large number of repeated loadings. Data of this type for a silty clay specimen subjected to a stress of 3 kg per sq cm at a frequency of 20 applications per min have been obtained from Seed and Chan (17) and plotted on an arithmetic scale as shown in Figure 32. These same data have then been plotted on a hyperbolic test plot in Figure 33. A hyperbola provides a very good fit for the data within a certain range, but no one hyperbola satisfies the full range of the test data. Thus, the strain must be given as

$$\epsilon = \frac{N}{1.25 + N} \text{ for } 3 \leq N \leq 500 \quad (11)$$

$$\epsilon = \frac{N}{175 + 0.6N} \text{ for } 500 \leq N \leq 10,000 \quad (12)$$

dependent only on the number of stress applications.

A review of the literature on repeated loading of bearing plates revealed a general scarcity of test data representing a large number of load applications. Many authors tread on dangerous ground by extrapolating the results of a few tests with a small number of load applications to predict the probable results at thousands of times the actual recorded data with the assumption of an exponential re-

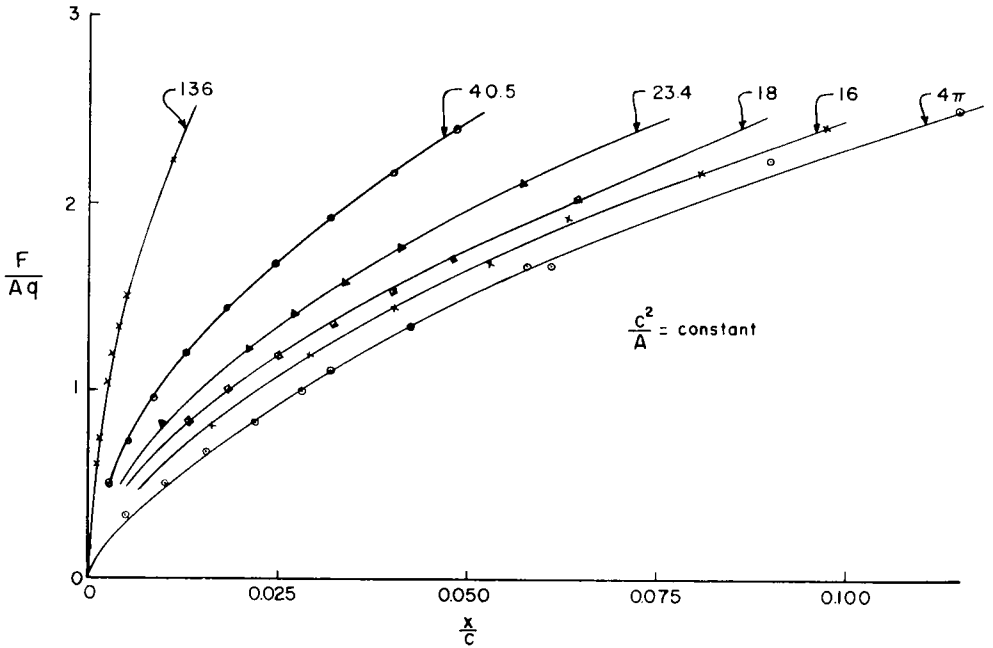


Figure 26. Nondimensional plot of  $x/C$  vs  $F/Aq$  for constant value of  $C^2/A$ .

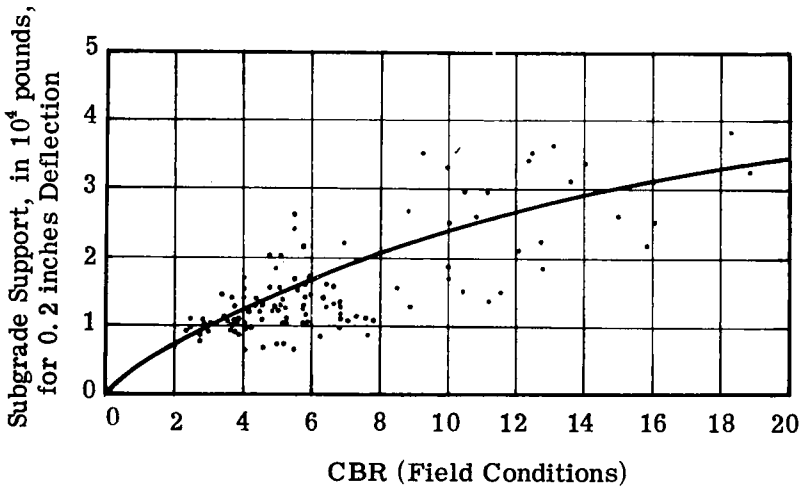


Figure 27. Subgrade support vs field California bearing ratio.

It can be verified that these data are also not satisfied over the full range by an exponential expression.

Another set of data obtained from Seed, Chan, and Monismith (18) is

for a silty clay specimen subjected to triaxial compression with a constant lateral stress of 14.2 psi and an axial stress of 40 psi applied 10 times per min for a period of 1 sec each time.

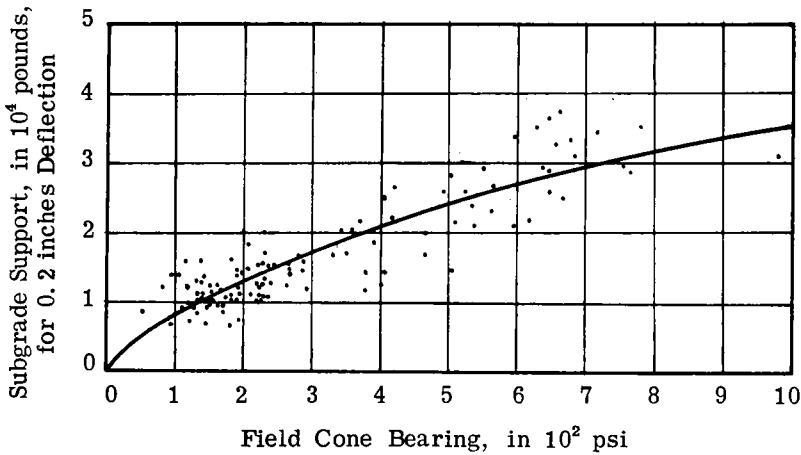


Figure 28. Subgrade support vs field cone bearing.

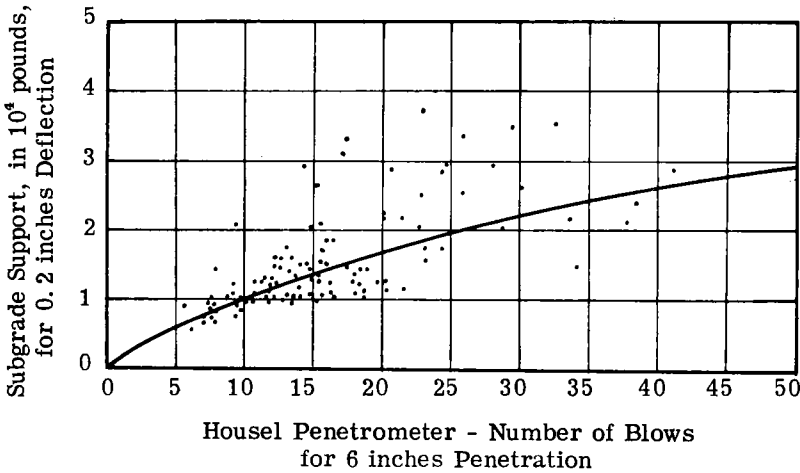


Figure 29. Subgrade support vs Housel penetrometer.

These data satisfy very well the hyperbolic test plot as shown in Figure 34 and again reveals the necessity of fitting each range with a separate hyperbola.

$$\epsilon = \frac{N}{4 + 3.2N} \text{ for } 3 \leq N \leq 500 \quad (13)$$

$$\epsilon = \frac{N}{550 + 1.92N} \text{ for } 500 \leq N \leq 10,000 \quad (14)$$

Thus, it appears that a hyperbola provides a very good fit for repetitional test data within a certain range. The test plots in each case indicate the slope of the line representing the 500 to 10,000 range to be about 60 percent of the slope of the line for the 3 to 500 range. It is possible that analysis of additional data will verify a definite relationship between these two hyperbolas. If so, this would provide a rational basis to

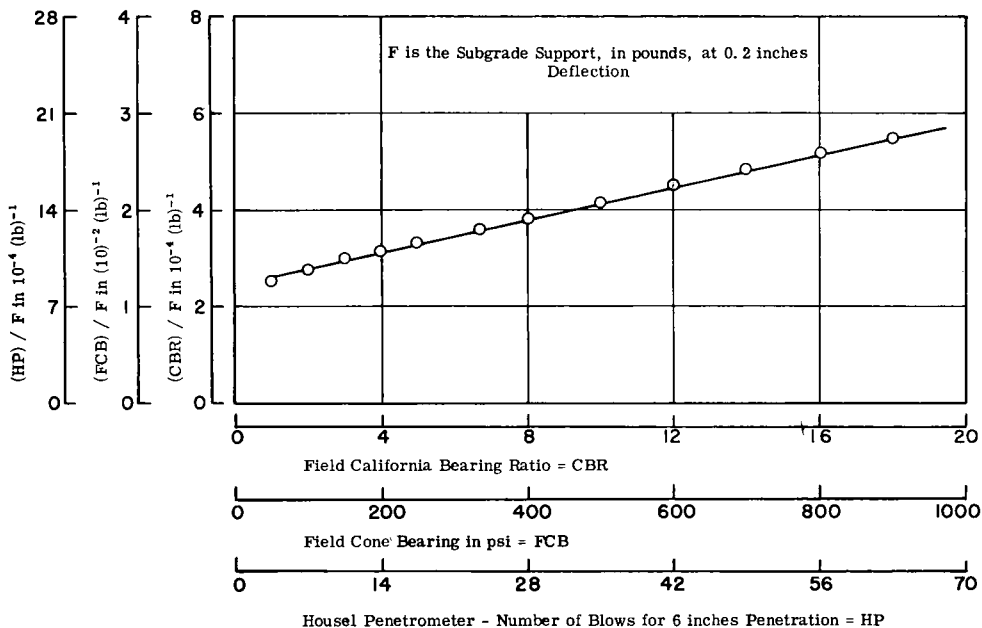


Figure 30. Correlation of plate bearing tests and various soil strength indexes.

extrapolate the results of the low range to the higher range.

CONCLUSIONS

The investigation reported in this paper leads to the following conclusions:

1. The phenomena of rigid bearing plate tests on soil can be described in functional form as

$$\frac{x}{C} = \kappa \left( \frac{F}{Aq}, \frac{C^2}{A}, \frac{Ft}{A\eta}, N, \phi \right) \quad (3)$$

2. Load test procedures influence the applied stress vs deflection relation through the effects of the term  $Ft/A\eta$ .

3. Model and field bearing plate test results can be represented by the two-constant hyperbolic form

$$\frac{F}{A} = \frac{\frac{x}{C}}{a + b \frac{x}{C}} \quad (7)$$

4. Laboratory stress-strain tests, conducted on several of the same soils tested with bearing plates, can be expressed as

$$\sigma = \frac{\epsilon}{a + b\epsilon} \quad (8)$$

Comparison of conclusions 3 and 4 tends to substantiate the concept that a soil strength parameter is "built into" the shape of the load-deflection curve for a plate bearing test; that is, the shape of the curve is dictated by the strength characteristics of the soil.

5. California bearing ratio test results can also be expressed in the form of Eq. 7, indicating a correlation with plate bearing tests. Thus, the CBR value is a ratio of the soil strength parameter to the strength parameter of a standard reference material; namely, crushed stone at a particular value of  $x/C$ .

6. The influence of the shape of the bearing plate is given by the varia-



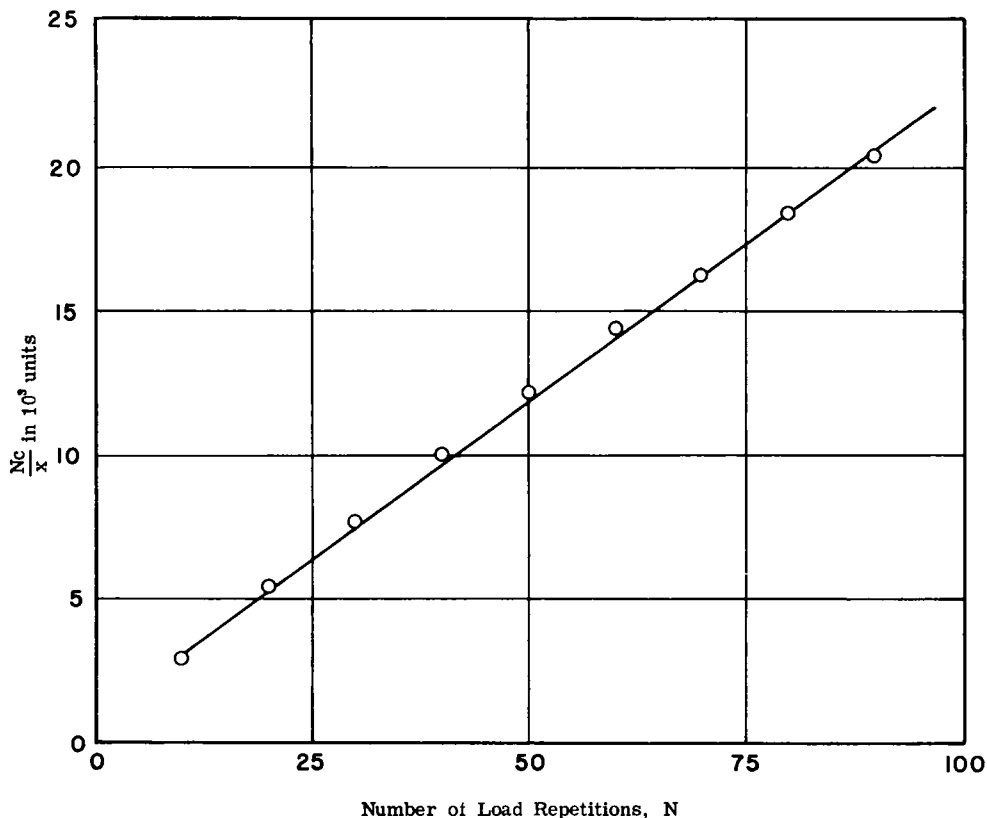


Figure 31. Bearing plate tests, load repetitions (McLeod).

tion of  $C^2/A$ , where  $C$  is the perimeter and  $A$  is the cross-sectional area.

7. A hyperbolic relation can be used to correlate plate bearing tests and field cone-bearing, Housel penetrometer, and California bearing ratio tests.

8. The results of repetitional load bearing and repetitional laboratory stress-strain tests can be expressed in the hyperbolic forms

$$\frac{x}{C} = \frac{N}{a + bN} \text{ for } \alpha \leq N \leq \beta \quad (10)$$

and

$$\epsilon = \frac{N}{a + bN} \text{ for } \bar{\alpha} \leq N \leq \bar{\beta} \quad (11)$$

where the constants  $a$  and  $b$  depend on the range of  $N$  considered.

#### ACKNOWLEDGMENTS

The authors wish to express their appreciation to Jorj O. Osterberg, Professor of Civil Engineering, Northwestern University, for his assistance in providing some of the experimental data used in the analysis and for his general encouragement.

The authors are also indebted to the many researchers whose published test results have been analyzed in this paper.

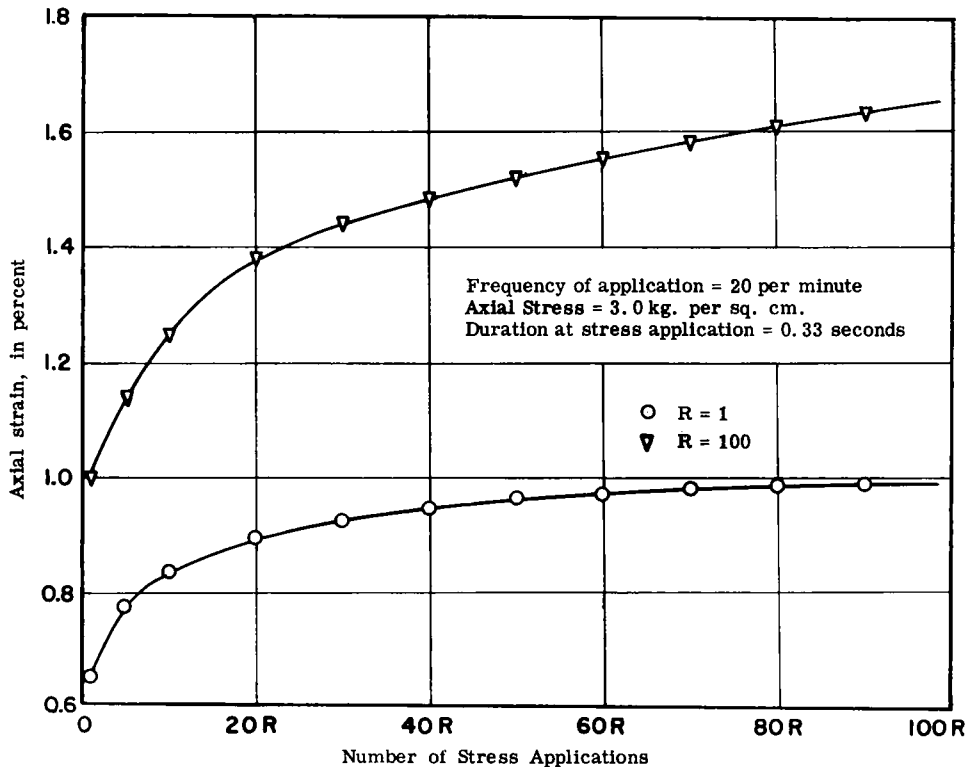


Figure 32. Axial strain vs number of stress applications (Seed and Chan).

#### REFERENCES

- HOUSEL, W. S., "Final Report—Symposium on Load Tests of Bearing Capacity of Soils." ASTM Special Tech. Publ. 79 (June 1947).
- TERZAGHI, C., "The Science of Foundations—Its Present and Future." *Trans., ASCE*, 93: 392 (1929).
- KONDNER, R. L., "A Non-Dimensional Approach to the Vibratory Cutting, Compaction and Penetration of Soils." The Johns Hopkins University, Department of Mechanics, Tech. Rept. 8 (Aug. 1960).
- KONDNER, R. L., AND EDWARDS, R. J., "The Static and Vibratory Cutting and Penetration of Soils." *HRB Proc.*, 39: 583-604 (1960).
- KONDNER, R. L. AND KRIZEK, R. J., "A Non-Dimensional Approach to the Static and Vibratory Loading of Footings." *HRB Bull.* 277: 37-60 (1960).
- KONDNER, R. L., "Non-Dimensional Techniques Applied to Penetrometer Studies in Cohesive Soils." ASTM (1961). (In press)

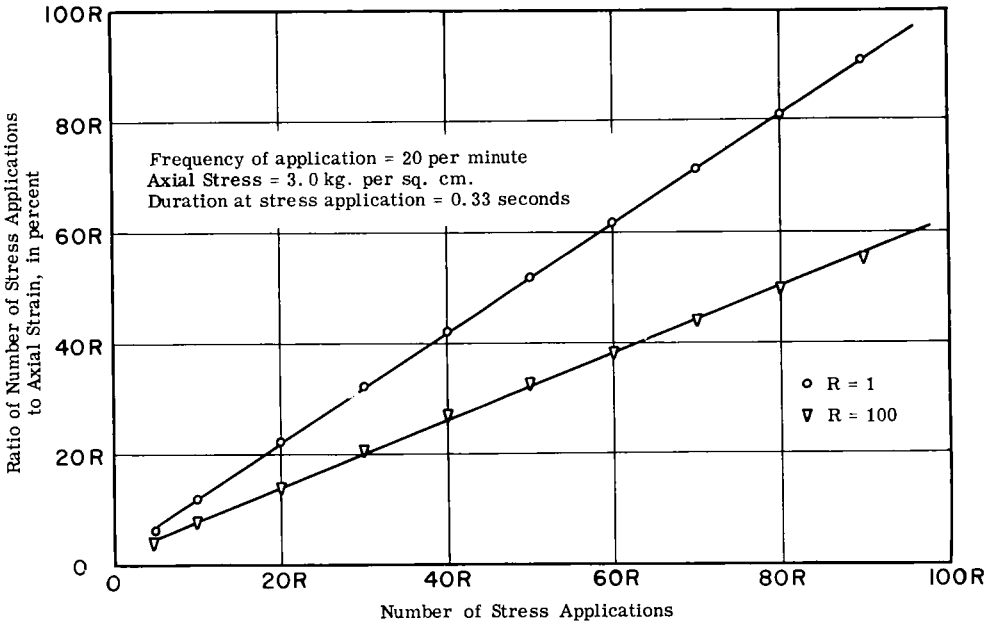


Figure 33. Axial strain vs number of stress applications (Seed and Chan).

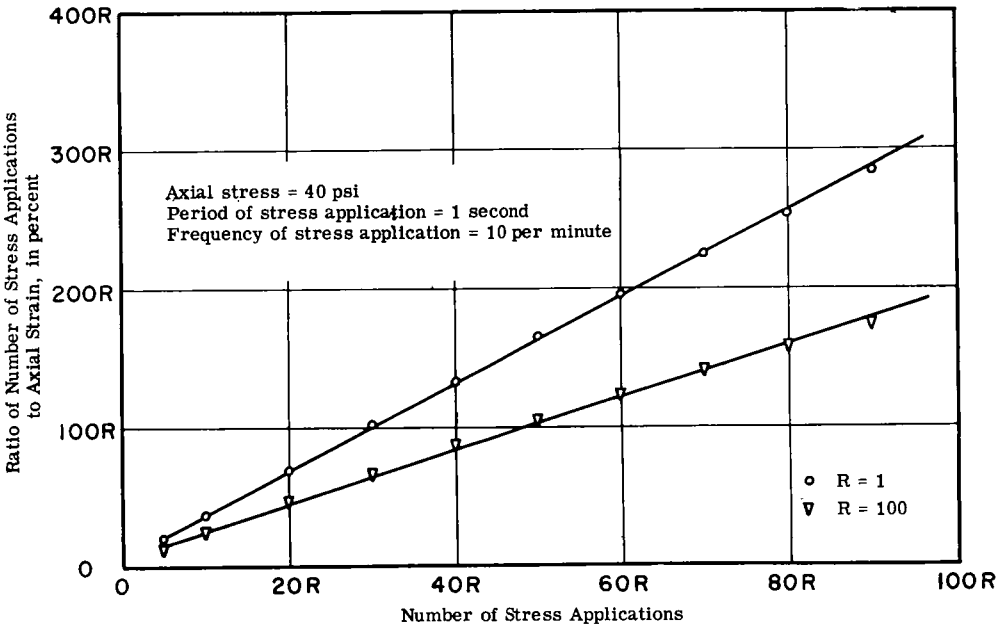


Figure 34. Axial strain vs number of stress applications (Seed, Chan, and Monismith).

7. KONDNER, R. L., "A Study of the Bearing Capacity of Vertically Loaded Friction Pile Groups in Cohesive Soil." ASCE, (1961). (In press)
8. KONDNER, R. L., "Non-Dimensional Techniques in Soil Mechanics." Soil Mechanics and Foundation Div., ASCE, (1962). (In preparation)
9. KONDNER, R. L., AND GREEN, G. E., "Lateral Stability of Rigid Poles Subjected to Ground-Line Thrust." HRB Bull. 342. (In press)
10. BRIDGMAN, P. W., Dimensional Analysis." New Haven (1931).
11. LANGHAAR, H. L., "Dimensional Analysis and Theory of Models." New York (1951).
12. DIX, H. J., AND LUKAS, R. G., "A Comparison of Observed Performance with the Predicted Behavior of Plate Bearing Tests on a Chicago Clay." M. S. Thesis, Northwestern Univ. (July 1959).
13. BENKELMAN, A. C., AND WILLIAMS, S., "A Cooperative Study of Structural Design of Nonrigid Pavements." HRB Special Report 46 (1959).
14. OSTERBERG, J. O., "Discussion—Canadian Investigation of Load Testing Applied to Pavement Design." ASTM Special Tech. Publ. 79 (June 1947).
15. MCLEOD, N. W., "Canadian Investigation of Load Testing Applied to Pavement Design." ASTM Special Tech. Publ. 79 (June 1947).
16. PORTER, O. J., "Development of the Original Method for Highway Design." *Trans., ASCE*, Vol. 115 (1950).
17. SEED, H. B., AND CHAN, C. K., "Thixotropic Characteristics of Compacted Clays." *Proc., ASCE*, Vol. 83 (Nov. 1957).
18. SEED, H. B., CHAN, C. K., AND MONISMITH, C. L., "Effects of Repeated Loading on the Strength and Deformation of Compacted Clay." *HRB Proc.*, 34: 541-558 (1955).

## DISCUSSION

G. RAGNAR INGIMARSSON, *Research Assistant, Soil Mechanics Laboratory, University of Michigan, Ann Arbor.*—This discussion is limited mainly to the authors' conception of Eqs. 6 and 8 and the use of experimental results in support thereof.

An explicit form of the  $F/A$  vs  $x/C$  relation for bearing plate tests is

$$\frac{x}{C} \frac{A}{F} = a + b \frac{x}{C} \quad (6)$$

Specific bearing plate tests by Dix and Lucas are shown in Figure 9,

and the results plotted as  $\frac{x}{C} \frac{A}{F}$  vs  $\frac{x}{C}$

in Figure 10. The writer has taken

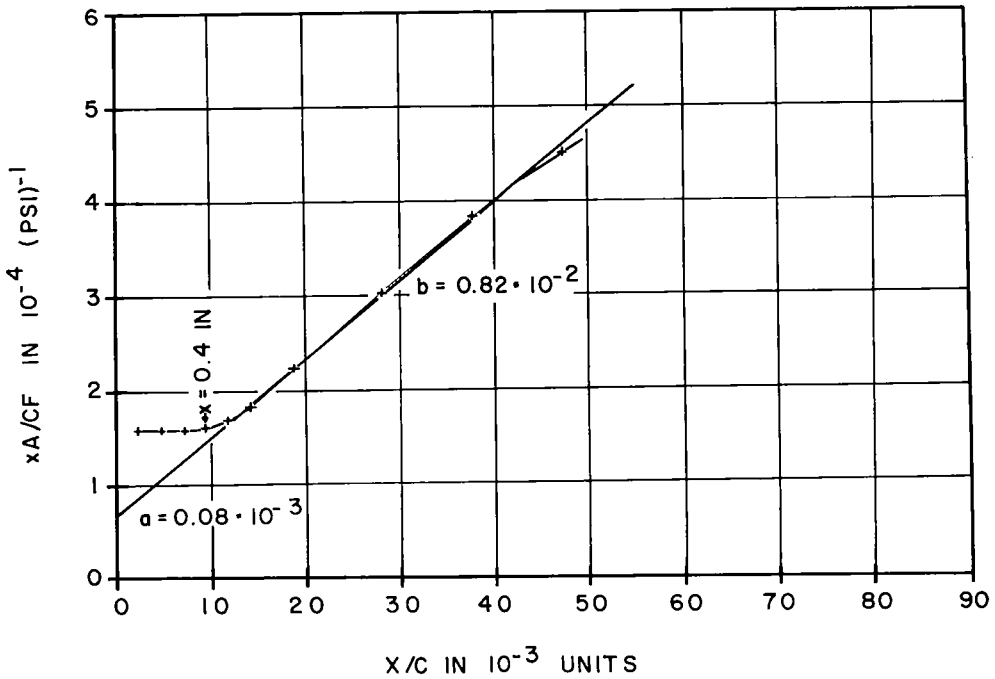


Figure 35.

the results for Plate 1 as presented in Figure 9 and given the values for  $x$ ,  $x/C$ , and  $A/F$  in Table 3. Values of  $\frac{x}{C} \frac{A}{F}$  vs  $\frac{x}{C}$  are then plotted in Figure 35.

first point plotted in Figure 10 corresponds to  $x=0.4$  in., with all values of  $x < 0.4$  in. thus being neglected. Referring to Figure 35, it is evident that points from  $x=0$  in. up to  $x=0.5$  ft would be much better represented by an entirely different straight line from that shown in Figure 10.

Comparing Figure 10 and Figure 35, it cannot be overlooked that the

Because Eq. 6 can be rewritten

$$\frac{A}{F} = \frac{C}{x} a + b \tag{15}$$

representing a straight line when  $A/F$  is plotted vs  $C/x$ , values of  $a$  and  $b$  could be obtained as the slope of the line and the intercept with the vertical axis, respectively. This plot

has the advantage over the  $\frac{A}{F} \frac{x}{C}$  vs  $\frac{x}{C}$  plot in that the values plotted do

TABLE 3<sup>1</sup>

$x$ (in)	$x/C$	$A/F$
0.1	0.00236	0.067
0.2	0.00472	0.083
0.3	0.00708	0.022
0.4	0.00943	0.017
0.5	0.01180	0.014
0.6	0.01416	0.013
0.8	0.01886	0.012
1.2	0.02832	0.011
1.6	0.03772	0.010
2.0	0.04718	0.009

<sup>1</sup>  $D=13.5$  in.;  $C=42.4$  in.;  $1/C=0.0236$ .

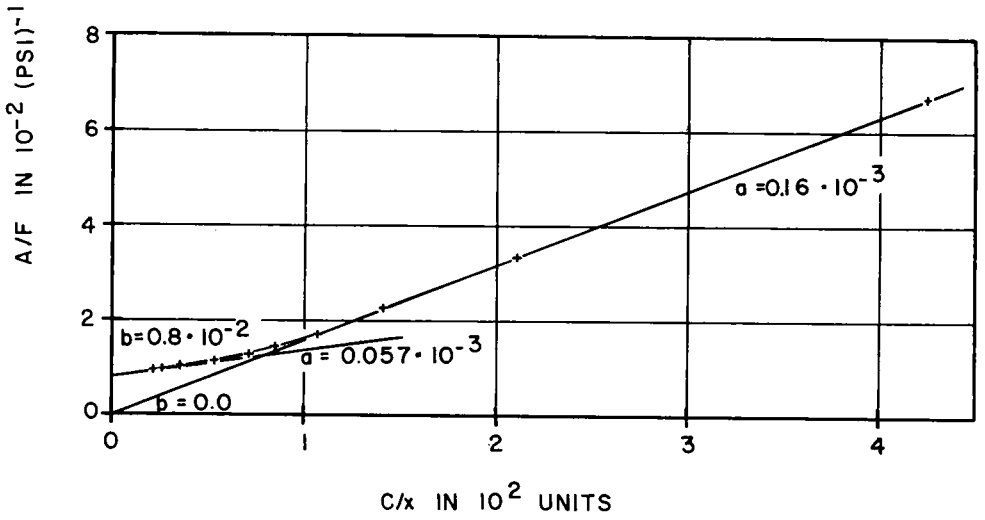


Figure 36.

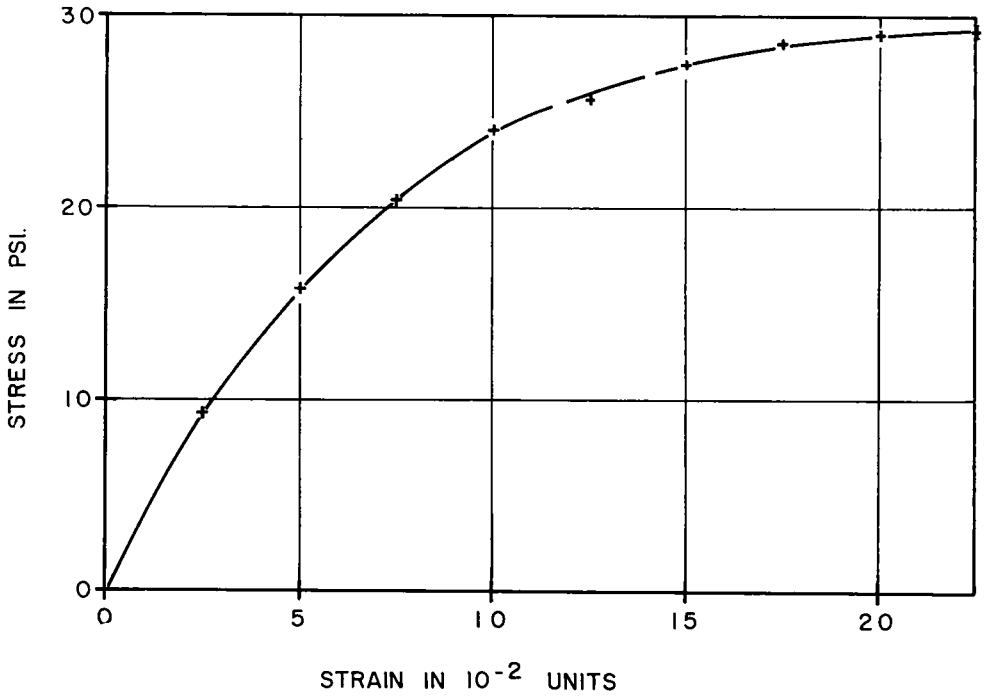


Figure 37.

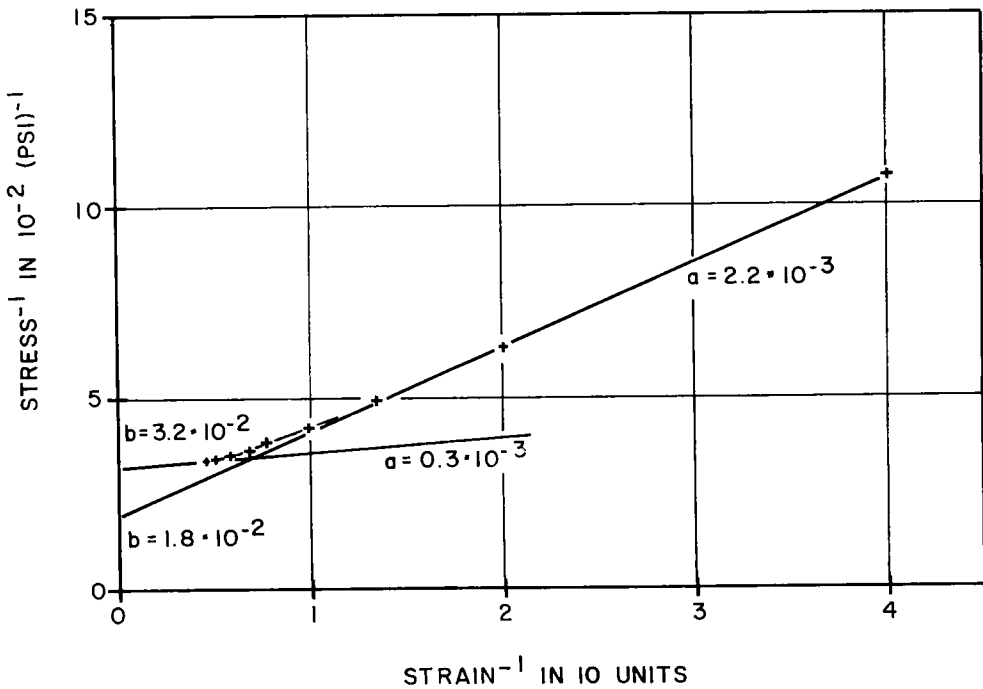


Figure 38.

not have a common factor,  $x/C$ , hence are less liable to give a deceiving picture of the correlation between the variables.

The data from Figure 9 have been replotted in Figure 36 as  $\frac{A}{F}$  vs  $\frac{C}{x}$ .

It will be noted that the points do not represent a straight line but rather a curve. Tangents to this curve would give values of  $a$  anywhere from  $0.057 \times 10^{-3}$  to  $0.16 \times 10^{-3}$ , and of  $b$  from 0 to  $0.8 \times 10^{-2}$ .

The authors further suggest that the stress-strain relation obtained from laboratory testing may be represented by

$$\sigma = \frac{\epsilon}{a + b\epsilon} \quad (8)$$

In support of this suggestion, results from an unconfined compression test are shown in Figure 11 as  $\frac{\epsilon}{\sigma}$  vs  $\epsilon$ . A straight line is drawn through the points, giving  $b$  and  $a$  as the slope of the line and intercept with the vertical axis, respectively.

For the purpose of reference, the stress-strain curve for Plate 1 for the unconfined compression test has been reconstructed on the basis of the data given in Figure 11 and is shown in Figure 37.

Reviewing the data in Figure 11, it is felt rather questionable to represent the plotted points by a straight line inasmuch as they consistently form a smooth curve rather than being scattered at random around a straight line. To further demonstrate this point, Eq. 8 can be rewritten as

$$\frac{1}{\sigma} = a \left( \frac{1}{\epsilon} \right) + b \quad (16)$$

and the results plotted up as  $\frac{1}{\sigma}$  vs  $\frac{1}{\epsilon}$ .

This has been done in Figure 38 for the same points as shown in Figure 11. Depending on which portion of the curve is considered, straight lines represented by  $a$  and  $b$  varying in value from  $0.3 \times 10^{-3}$  to  $2.2 \times 10^{-3}$  and from  $1.8 \times 10^{-2}$  to  $3.2 \times 10^{-2}$ , respectively, can be selected.

On the basis of this discussion, the writer concludes that the authors' Eqs. 6 and 8 do not adequately describe the entire range of the load-deflection or stress-strain relationship. Particularly, the equations as presented are not valid over the initial portion of the load-deflection curve. It is the initial portion of this curve which is of concern to the designing engineer.

ROBERT L. KONDNER AND RAYMOND J. KRIZEK, *Closure*.—The authors wish to thank Mr. Ingimarsson for the opportunity to demonstrate the applicability of the analysis presented. It is perhaps appropriate to state at the outset that no "exact" fit of experimental data is presented in this paper nor was there the intention to do so. Because of the complexity of soil as a structural material with its observed viscoelastic type of response and the general difficulty of problems involving the interaction of soil-solid systems, as well as the complications that arise as a result of current test procedures (discussed under "Rate Effects") plus experimental error, it is unreasonable to expect an "exact" fit to assume such a simplified analytic nature as a two-constant hyperbola. Eqs. 6 and 8 have been proposed by the authors as a reasonable fit over a large range of the deflection

parameter for the experimental bearing plate and stress-strain test data examined.

Regarding the Dix and Lukas test data for Plate 1, Mr. Ingimarsson points out in Figure 35 that all of the experimental points do not lie exactly on a straight line in the hyperbolic test plot. This is evident in Figure 10. In Figure 36, he replots this same data in what he refers to as a less "deceiving picture of the correlation between the variables" and then proceeds to point out the variety of straight lines that may be passed through these data. First, in Figure 36, as the force,  $F$ , and the deflection,  $x$ , go to zero, the variables plotted go to infinity; thus, the test data from  $x=0$  to  $x=0.3$  in. in Figure 9 lie in the abscissa range from 1.41 units to infinity in Figure 36 whereas the remaining 88 percent of the data is plotted in the relatively small region from 0 to 1.41 units. The authors feel, therefore, that Figure 36 represents the more deceiving plot and submit in support thereof the fact that it becomes much more difficult to exercise objectively the engineering judgment required to fit the data with the "best" straight line. The prevailing tendency with Figure 36 is to weight the relatively small portion of the initial data (low values of force vs deflection) too heavily because it extends to infinity. As an example, if the "best straightline" fit of the data in the Figure 36 were chosen as the line represented by  $a=0.16 \times 10^{-3}$  and  $b=0.0$ , one of the possibilities suggested by Mr. Ingimarsson, this would imply that the ultimate stress  $F/A$  which may be applied to Plate 1

would be infinite  $\left[ \left( \frac{F}{A} \right)_{\text{ult}} = \frac{1}{b} \right]$ . In

his discussion, Mr. Ingimarsson has emphasized the initial portion of the data and his plot of  $A/F$  and  $C/x$



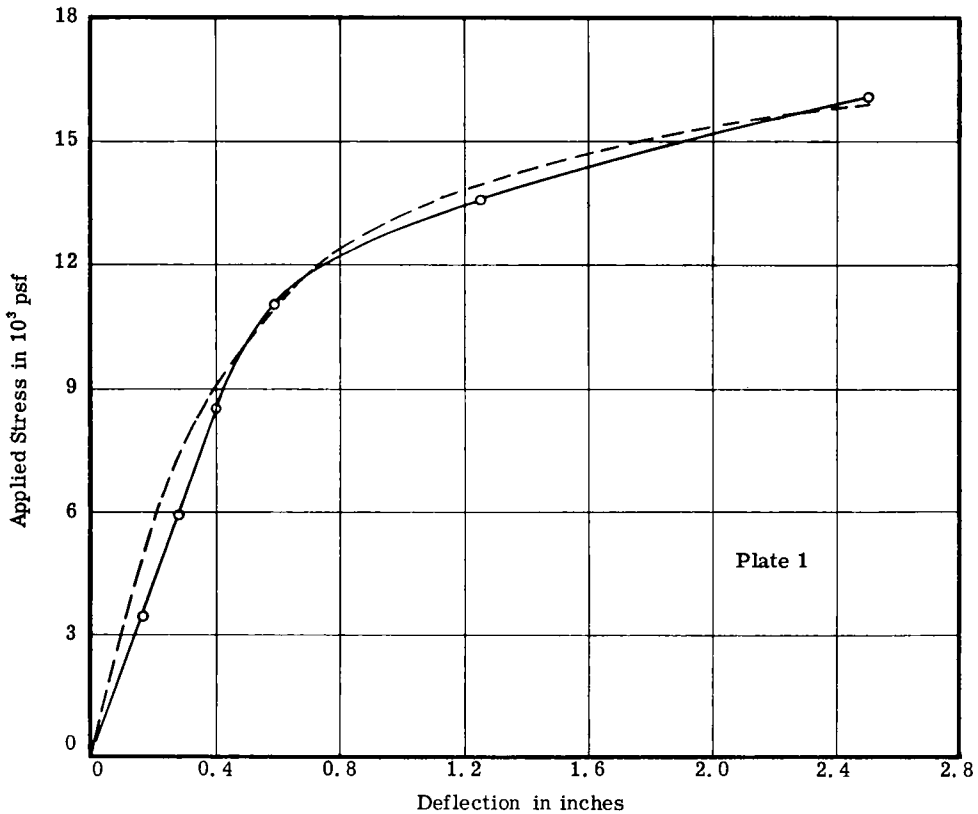


Figure 39.

strongly reflects this emphasis; however, careful examination of the nature of a hyperbolic fit will reveal that any tendency to emphasize the significance of data in the initial region will be accompanied by a corresponding overestimation of the ultimate values and this is, of course, on the unsafe side, as has been previously evidenced. In addition, the data from the initial portion of a test are often less reliable than the data from the remainder of the test due to such uncertainties as seating effects. This is particularly true for the data from Plate 1 inasmuch as the test was conducted 20.6 ft beneath the ground surface where control was less rigid.

The "best straight line" as selected by the authors yields a prediction curve as shown by the dashed line in Figure 39 as compared to the actual data represented by the solid line. In light of the explanation presented, it is felt this provides a reasonable representation of the actual results obtained.

Essentially similar comments may be expressed concerning Mr. Ingimarsson's discussion of the stress-strain data presented in Figure 11 for Plate 1. Figure 38 is analogous to Figure 36 in the method of plotting. The results of the authors' fit for these data (from Fig. 11) is superimposed on Figure 37 and shown

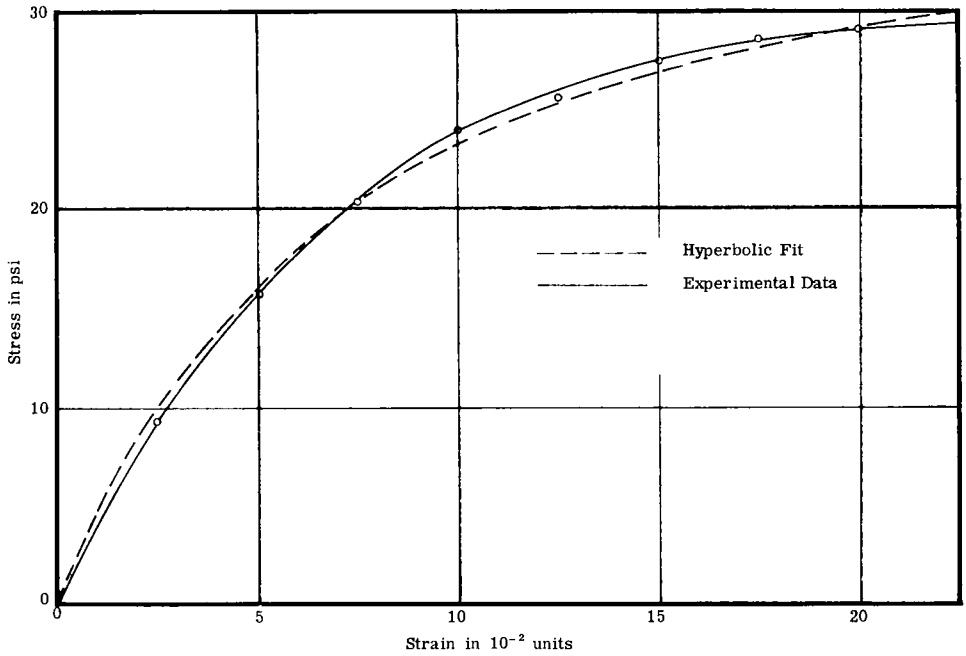


Figure 40.

as Figure 40. The close agreement between actual test data and the proposed hyperbolic fit is apparent.

In summary, Eqs. 6 and 8 are not suggested as "exact" fits for all test data, but only as good approxima-

tions over a large range of the deflection parameter for the data examined. This is felt to have been demonstrated in Figures 39 and 40, hence the authors feel the conclusions of the paper to be justified.